Evaluation and Improvement of the PIEKTUK Blowing Snow Model on the Canadian Prairies and Arctic

by

James Edward Butler

A thesis submitted to the Faculty of Graduate Studies in partial fulfillment of the requirements for the degree of

Master of Science

Centre for Earth Observation Science
Department of Environment & Geography
University of Manitoba

Winnipeg. Manitoba, Canada, 2008

THE UNIVERSITY OF MANITOBA

FACULTY OF GRADUATE STUDIES
*****
COPYRIGHT PERMISSION

Evaluation and Improvement of the PIEKTUK Blowing Snow Model on the Canadian Prairies and Arctic

BY

James Edward Butler

A Thesis/Practicum submitted to the Faculty of Graduate Studies of The University of

Manitoba in partial fulfillment of the requirement of the degree

Of

Master of Science

Abstract

Blowing snow is an important part of Canadian's lives. Accurate forecasting of blowing snow events and their visibility can be an important factor for the safety of Canadians. The PIEKTUK blowing snow model can be used to predict the occurrence of blowing snow, and to predict the visibility during an event. During an initial analysis, the model appeared to predict the occurrence of blowing snow very accurately, but once null weather events were removed, the model over-predicted more events than it correctly forecast. In an attempt to improve the forecasting capabilities of the model, the calculation for the threshold wind speed was tested by increasing and decreasing the constant coefficient in the equation incrementally to see if another value was optimal. For most stations, increasing the constant by 1 to 5 improved the forecasting of blowing snow events over the original version. More consistent improvements were found in Prairie and Arctic regions than in Forest or Mountain regions. The influence of wind direction was also added into the model, and the results were analyzed for one Prairie station and one Arctic station. Minimal improvement was observed for Winnipeg, and none for Baker Lake. The predictions made by PIEKTUK were also compared to data recorded during the CASES project. Unlike earlier conclusions, decreasing the constant by -2 was found to improve the model the most due to the smooth nature of the surface (snow covered first-year sea ice)..

Acknowledgements

I would like to thank my supervisor Dr. John Hanesiak for all his support and guidance during the writing of my thesis. I would also like to thank my committee, Dr. Tim Papakyriakou and Dr. Paul Bullock for their input and suggestions as to the direction of my thesis. Peter Taylor, Teresa Fisico, An Tat, Rob Pierson and Sergey Savelyev for their assistance in recording of weather observations and visibility measurements during the CASES project. Also my gratitude to all those who helped with the maintenance of the ice camp where the observations were recorded, of who there are too many to mention. I would also like to thank David Baggaley for providing the data from Environment Canada that allowed me to do my research and John Iacozza for assisting with the statistical analysis.

Dedication

This thesis is dedicated to my mother, Mona Butler, and my husband Lester Beaton for their support during the writing of my thesis. They kept me going during a few rough periods I encountered while I was writing it. I would also like to dedicate this thesis to my father, Edward Butler, who did not get to see the final result of my years in Graduate Studies. My thanks to my sister Kristine Dyck for forwarding all my messages to assorted friends and family and for keeping in touch with me while I was in the Arctic.

Table of Contents

List of Tables

List of Figures

1: Introduction

1.1 Importance of Research and Background

Blowing snow, which is defined by the Manual of Surface Weather Observations (MANOBS, 1990) as snow particles lifted by the wind to reduce horizontal visibility to six miles or less at eye level, is a part of life for most Canadians. It can have a significant effect on our lives, from forcing the rescheduling of outdoor events to completely stopping transportation. Blowing snow events can range from being a nuisance to endangering people's lives if they are not prepared for these events. Accurate forecasting of these events allow people time for preparation, whether it means leaving an hour earlier for a trip, to cancelling all travel plans and preparing to be isolated for a period of time. Inaccurate forecasting of severe events lowers people's level of trust in the forecasts, and may lead them into dangerous situations. Increasing the accuracy of the forecasts could greatly improve the lives of Canadians, especially those who live in areas prone to this type of weather phenomenon.

Wind is the most important parameter when it comes to blowing snow. The distribution of the particles of blowing snow in a given vertical space was explored by Mann et al. (2000) in their paper *Profile measurements of blowing snow at Halley, Antarctica*. Their research showed that the particle content at a given wind speed can differ greatly depending on the threshold wind speed needed to begin the event. They showed that both particle concentrations and particle sizes decreased as the height increased. They also discovered a near saturated layer of air close to the snow pack in longer blowing snow events, causing a reduction in the amount of sublimation over the course of the event as opposed to shorter events

Li and Pomeroy (1997a) studied the threshold wind speed of blowing snow in greater detail using standard meteorological observations and based some of their work on Ôura et al. (1967). Ôura et al. (1967) showed that the threshold wind speed for blowing snow increases as temperatures increase above -7°C, because of an increase in a quasi-liquid layer above that threshold. This layer increases the cohesion of snow particles, increasing the minimum threshold wind speed needed to initiate a blowing snow event. Conklin and Bales (1993) showed that the liquid layer was present at a temperature of -60°C. The thickness of the layer at that temperature was 3-30 nm. They also showed that the same layer is present on snow particles at -1°C, with an increased thickness to 500-3000 nm. The thickness of the layer increased in a non-linear fashion as the temperature increased, and it increased rapidly as the temperature rose above -8°C (Conklin and Bales, 1993).

Li and Pomeroy (1997a) found that the threshold wind speed for blowing snow increased as the temperature increased from approximately -25°C, and the rate of the increase in threshold wind speed was more evident the warmer the air temperature. They also observed that at temperatures below -25°C the threshold increased as temperatures decreased (Figure 1.1).

Li and Pomeroy (1997b) also determined that the probability of blowing snow increases as temperatures decrease to -25°C, and after that point the probability decreases. Their data from that same study also suggested that the threshold wind speed for blowing snow events could be described by an equation using a constant, and temperature. The equation is:

$$U10t = 9.43+0.18*Ti+0.0033*Ti^2 \qquad (1.1)$$

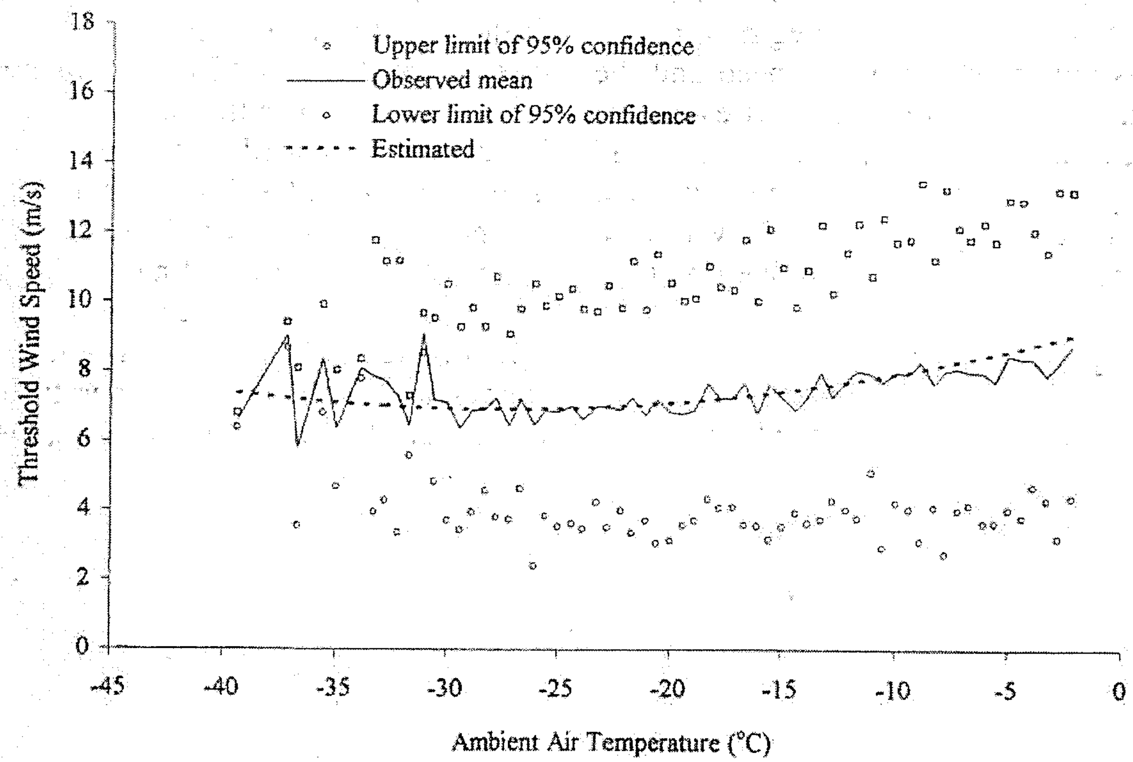

Figure 1.1 Estimated threshold wind speed and observed mean threshold wind speed: variation with ambient air temperature (Li and Pomeroy, 1997a).

They concluded using 6 years of observations that the threshold wind speed for a blowing snow event varies greatly even with the same air temperature, but average threshold wind speed is highly related to the air temperature (Li and Pomeroy, 1997a).

Once equations were developed to calculate when a blowing snow event would occur, models were developed to represent the physical process. Most of these models focused on the transport of snow, the amount of sublimation of snow, and changes to temperature and relative humidity during blowing snow events. A comparison of four of these models, PIEKTUK-B, PIEKTUK-T, WINDBLAST and SNOWSTORM, was preformed by Xiao et al. (2000). Their research focused on the different methods for predicting the sublimation and transport of snow, and the different results produced by them. The comparison of these models involved restricting surface variables, along with performing the model runs at night. Their study found that all of the models were sensitive to variables such as the initial temperature, relative humidity, and wind speed and particle size distribution.

Déry and Yau (2001a) attempted to combine the Canadian Mesoscale Compressible Community (MC2) with the PIEKUK blowing snow model to recreate blowing snow during a blizzard. They compared a run of the MC2 model by itself to a coupled run of the MC2 and PIEKTUK. The event they focused on was a strong low-level jet stream over Trail Valley Creek in the Canadian Arctic. Large amounts of blowing snow were present in such conditions. Their results showed that no actual precipitation fell in the region, and that all airborne snow was a result of blowing snow. The spatial distribution of blowing snow occurrence was captured reasonably well for their case study, however, no visibility analysis was preformed.

The main goal of other research has been to understand how blowing snow affects visibility. Blowing snow both scatters and absorbs electromagnetic energy, and the rate of both is relatively constant throughout the range of visible light (Pomeroy and Male, 1998). This allowed a formula of the meteorological definition of visibility, which is the distance a person with good vision, can distinguish a black object with a width of a 1° angle with their eye (Pomeroy and Male, 1998). Pomeroy and Male's (1998) formula calculated the visibility as:

$$V=3.912/\mu_{vis} \tag{1.2}$$

where V is in meters and μ_{vis} is the extinction coefficient for light at a wavelength of 600 nm. From this, it is possible to calculate the mean visual extinction efficiency by integrating it over various particle size distributions using a wavelength of 600nm (Pomeroy and Male, 1998). Research by Huang et al. (2007) found that particle size and distribution did not have a large effect on visibility. They also found correlation coefficients between wind speed and visibility as high as 0.93. Threshold wind speeds during the study were found to range between 5.5-7.9 m s^{-1} (Huang et al. 2007). They found that the Pomeroy and Male (1988) visibility model could be modified to relate blowing snow particle density at 1.5 m to visibility during a blowing snow event. Observed visibility during their study had a strong relationship to particle counter readings. They were able to use the relationship to predict visibility from particle counter readings, but warned that inaccurate particle counts and non spherical particles may cause some relative error.

Baggaley and Hanesiak (2005) looked at forecasting techniques in the Prairie Provinces and the Arctic. They found that 77.9% of blowing snow events on the Prairies involved precipitation while for Arctic stations that value was only 31.9%. They also found that for certain stations, blowing snow never occurred from certain wind directions. The highest critical success index was achieved by including the most variables in the forecasts. These variables included the highest air temperature since the past snowfall, snow age, and wind gusts (Baggaley and Hanesiak, 2005).

The process of blowing snow begins once the wind speed reaches a critical value (Déry and Yau, 1999). The time since the last snowfall, other precipitation events such as rain, the maximum temperature experienced by the snow pack, and the current temperature all play a role in this value. Snow transport can be broken down into three different processes. The first, creep, is the movement of snow particles along the ground. These particles are generally too heavy to be transported by the wind (Pomeroy and Goodison, 1997). The second method of snow transport is saltation. This method of transport occurs only in the first few millimetres of height, with the density of particles moved in this fashion decreasing exponentially with height (Pomeroy and Goodison, 1997). The final method of transport is by turbulent diffusion, or suspension of snow particles by the wind. Suspended snow particles are lifted by turbulent eddies from a few millimetres from the surface to 100 meters or more above the surface (Pomeroy and Goodison, 1997: Déry and Yau, 1999). Saltating snow particles are generally considered to be the source of suspended snow particles rather than surface snow crystals (Pomeroy et al, 1997).

1.2 Purpose of Research

The purpose of this thesis was to evaluate the effectiveness of the PIEKTUK blowing snow model at predicting the occurrence of blowing snow, and the accuracy of its visibility prediction with the primary goal of evaluating its potential use for improved operational blowing snow forecasts in the Canadian Prairies and Arctic.

1.3 Thesis Structure

Chapter 2 gives the climatology of Prairie, Arctic, Mountain, and Forest regions. A brief overview of the history of the PIEKTUK model is then presented (Chapter 3). The overall capability of the PIEKTUK model's ability to predict the occurrence of blowing snow was tested with a simple comparison between the model predictions and the observed data in Chapter 4. If they both showed blowing snow, or if both showed a null weather event, the model was correct. If the model predicted blowing snow, and none was observed, the model over-predicted the event. If there was a record of blowing snow, and the model missed it, the model under-predicted. Simple counts of this provided an initial analysis. The same process was then repeated excluding null weather events (Chapter 4). Also included in Chapter 4 is an initial assessment of the visibility predictions of PIEKTUK. Chapter 5 is devoted to the testing of the threshold wind speed, and to see if another value proves optimal (Section 1). The influence of direction was also added into the model in this chapter, and its usefulness examined (Section 2). In Chapter 6 the PIEKTUK model is evaluated against an Arctic data set that was collected during the 2004 CASES project. Chapter 7 restates all of my conclusions during my thesis, and suggests possible paths for future research.

2: Climatology of Blowing Snow

2.1 Introduction

The frequency of occurrence for blowing snow events varies between eco-climatic zones. In this chapter, complete wind patterns for two stations in each of the Prairie, Arctic, Forest, and Mountain eco-zones are shown. Also depicted, are the winds associated with severe blowing snow events. The severe events are divided into categories of between 1 and 3 statute miles (SM), 0.5 to 1 SM, 0.25 to 0.5 SM, and 0 to 0.25 SM.

2.2 Data and Methods

The data used for the climatology was provided by Environment Canada, and consisted of hourly observations from 26 weather stations across Western Canada and the Arctic. The observations were made from October 1st to March 31st. More detailed information on the data set used is provided in Chapter 3, Section 3. Two stations from each eco-climactic zone (Forest, Mountain, Prairie, and Arctic) were chosen. The data for these stations was reformatted using Climate Model, 8th revision created by Teresa Fisico (2003). This allowed the data to be fed into the Grapher 4 program. This program was used to create wind roses of all wind events, and also those which caused low visibility blowing snow events. A visual analysis of the wind roses was then preformed.

2.3 Arctic Regions

Arctic regions have the highest number of blowing snow events, due to their long winter season. Baker Lake is known as a location most prone to receiving such events. Over the course of the observed data (Table 2.1), a wind rose was created displaying every wind observation over the period (Figure 2.1). For this location, wind events are

Table 2.1 Blowing snow data and severe event observational counts.

Station Name	Starting Year of Observations (October - March)	Total Blowing Snow Events Observed	Severe Blowing Snow Events (Blowing Snow Only)	A	B	C	D
Baker Lake	1960	29789	12001	5911	1729	1666	2695
Resolute	1960	23669	9734	2183	1557	2177	3817
Winnipeg	1960	4514	952	28	77	216	631
Saskatoon	1960	2499	277	14	11	65	187
Fort Simpson	1963 (Nov)	1120	93	1	2	18	72
Fort Smith	1960	1181	215	1	5	29	180
Edmonton	1961 (Jan)	863	71	2	4	11	54
Red Deer	1960	893	73	7	10	10	46

predominantly from the north. Over the timeframe the data was collected there were 29,789 blowing snow events, with 12,001 of these events being severe events with only blowing snow affecting visibility. In this case, an event is defined as severe when the visibility is less than 3 statue miles (SM). These events are further broken down into 4 subcategories. Category A includes events with observed visibility of 0.25 SM or less. Category B contains events 0.5 SM or less, but greater than 0.25 SM. Category C contains events greater than 0.5 SM but less than or equal to 1 SM. The final category, D, contains the events between 1 SM and 3 SM. The wind pattern associated with these categories is displayed in Figure 2.2. The pattern for the wind direction and speeds for the severe blowing snow events is consistently from the north and northwest, with all wind speeds being 20 km h^{-1} or greater. There are very few events from any other direction for this station.

As another example of Arctic climatology, the observations from Resolute are also shown. The hourly observations from Resolute show more variation in the wind direction than Baker Lake, with some winds from the southeast, and some from the northeast (Figure 2.3). There were 23,669 blowing snow events during the observed period with 9734 of these events being severe blowing snow events. A specific wind rose for each of the separate visibility categories for this station is displayed in Figure 2.4. Unlike Baker Lake, the most common direction for blowing snow events is from the southeast and east. With so few wind events from the east, it is surprising that the percentage of severe events from that direction is so large.

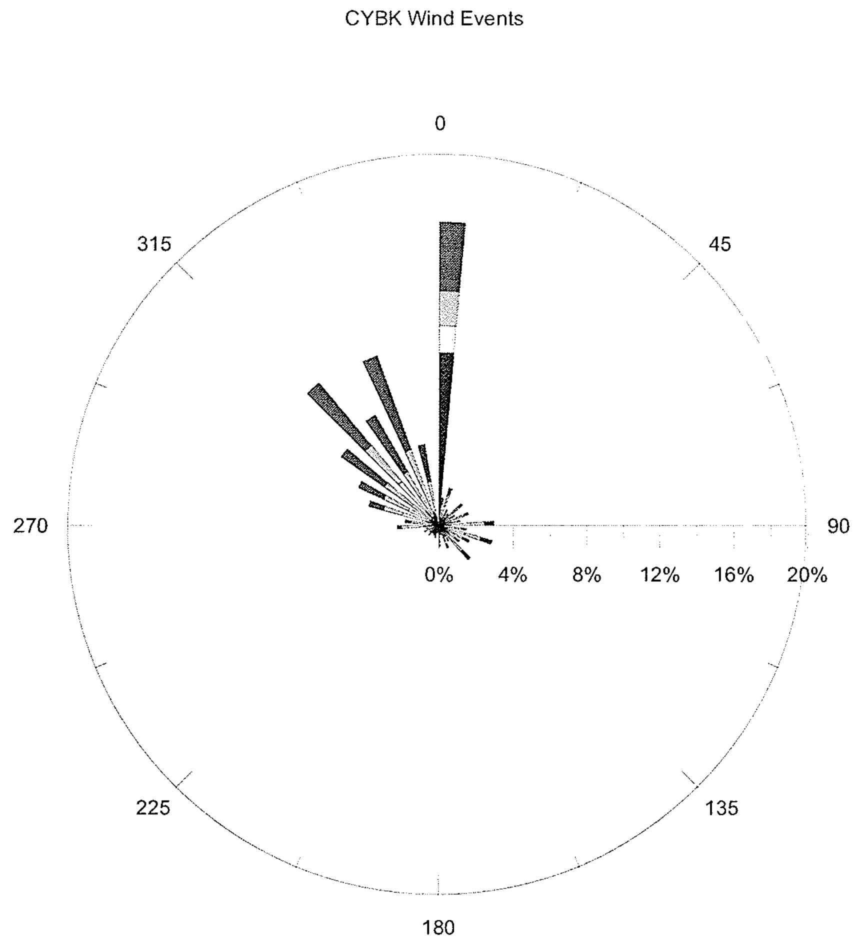

Figure 2.1 Complete wind data for Baker Lake. Blue sections in the chart show wind speeds less than or equal to 10 km h^{-1}, yellow 10 to 20 km h^{-1}, green 20 to 30 km h^{-1}, and red greater than 30 km h^{-1}.

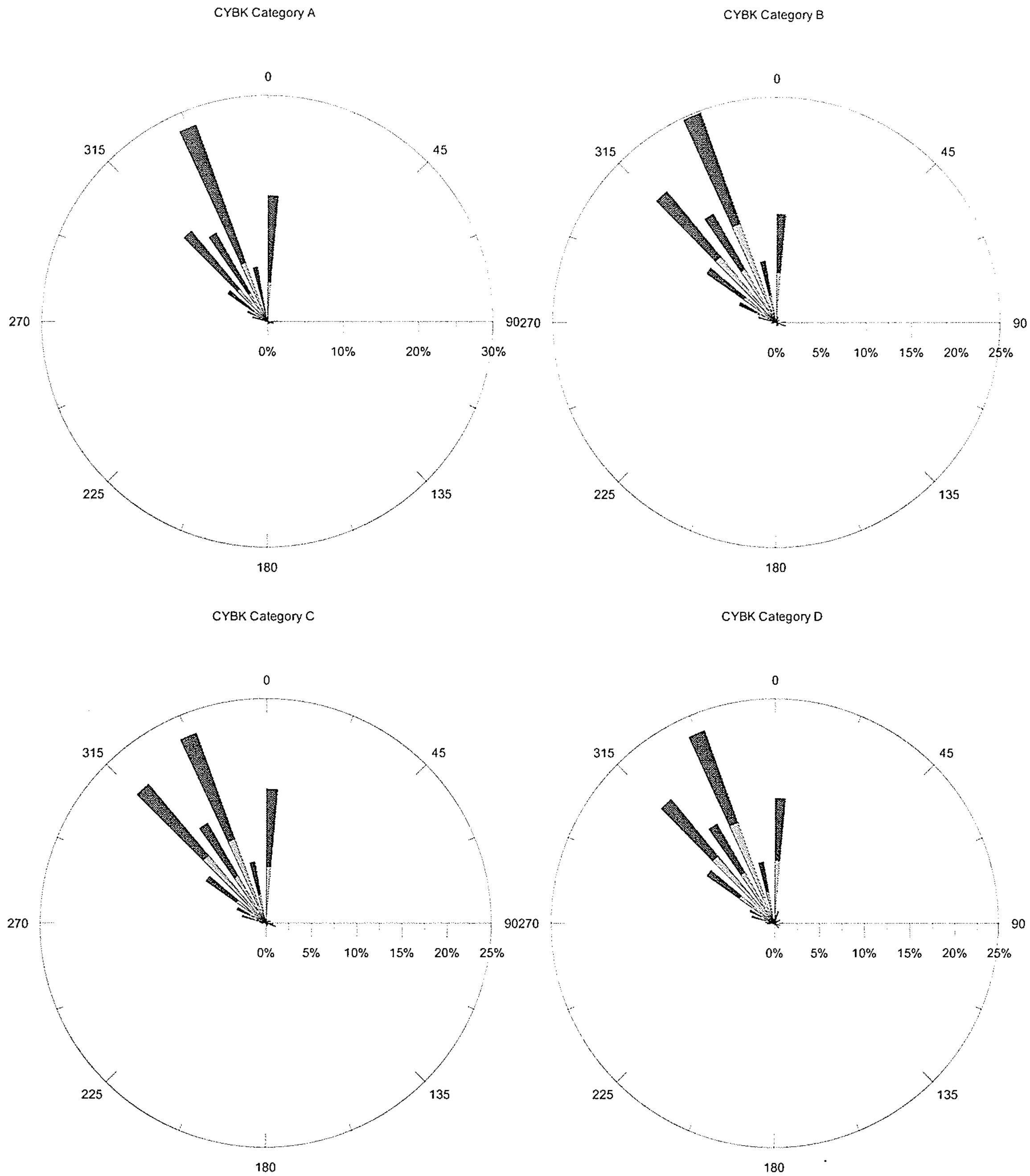

Figure 2.2 Wind roses for each category of severe blowing snow events for Baker Lake. Blue sections in the chart show wind speeds less than or equal to 10 km h^{-1}, yellow 10 to 20 km h^{-1}, green 20 to 30 km h^{-1}, and red greater than 30 km h^{-1}.

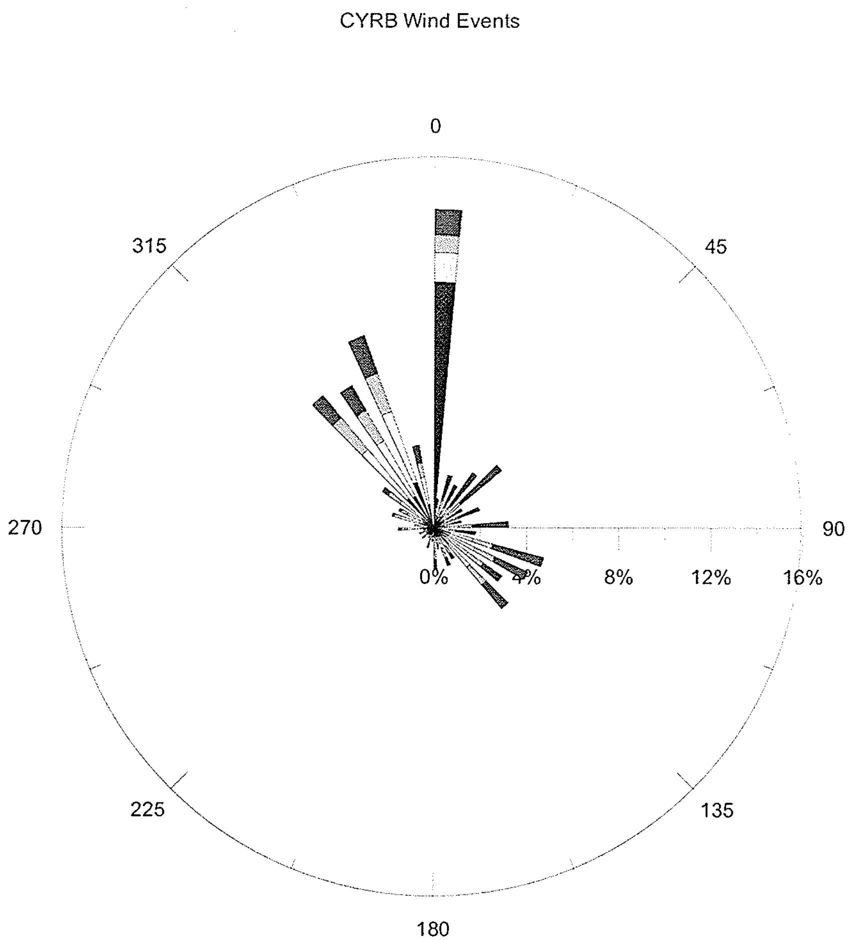

Figure 2.3 Complete wind rose for Resolute. Blue sections in the chart show wind speeds less than or equal to 10 km h^{-1}, yellow 10 to 20 km h^{-1}, green 20 to 30 km h^{-1}, and red greater than 30 km h^{-1}.

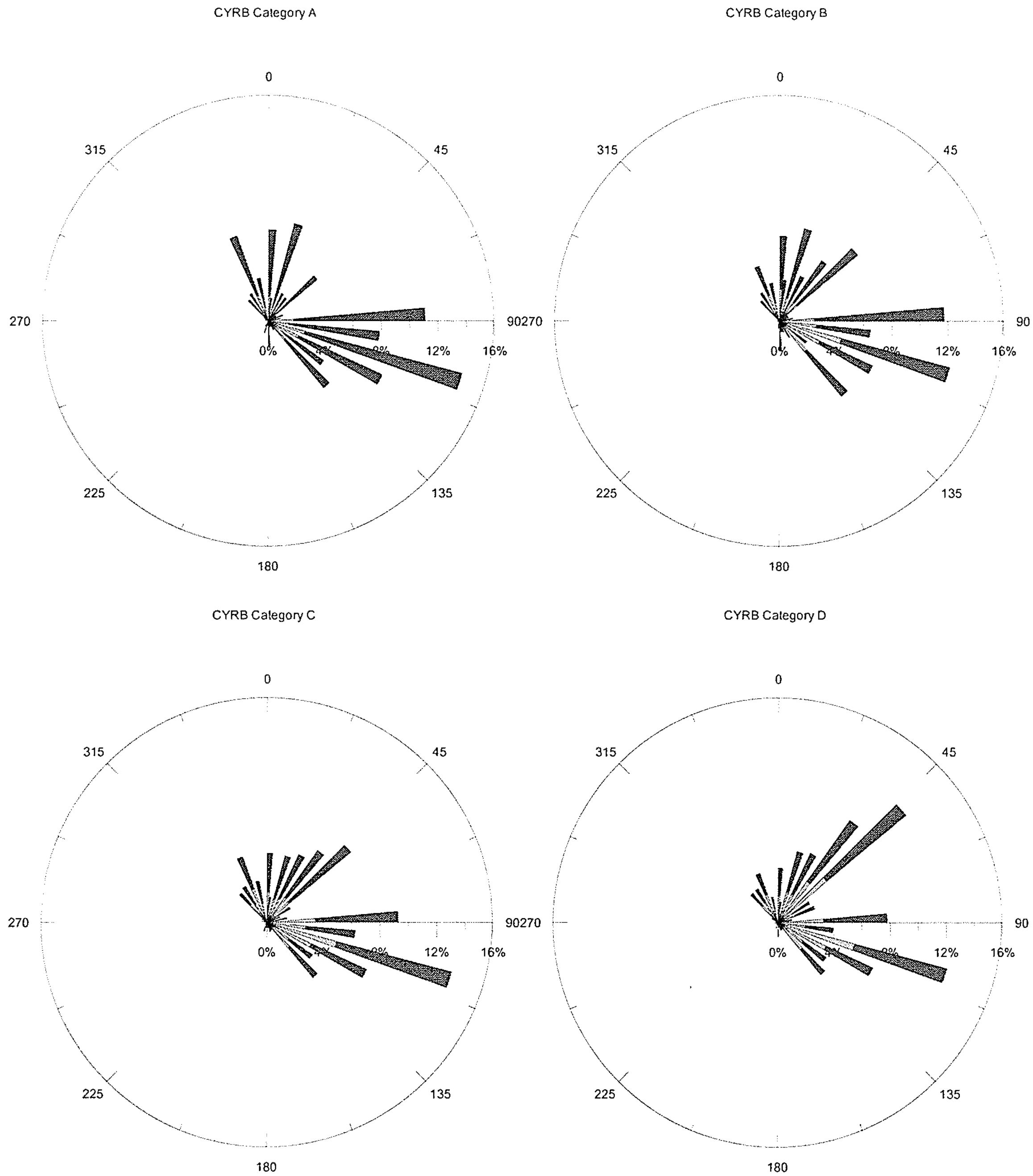

Figure 2.4 Wind roses for each category of severe blowing snow events for Resolute. Blue sections in the chart show wind speeds less than or equal to 10 km h^{-1}, yellow 10 to 20 km h^{-1}, green 20 to 30 km h^{-1}, and red greater than 30 km h^{-1}.

2.4 Prairie Regions

Winnipeg has a number of blowing snow events during the winter. Unlike the Arctic stations, the wind events come from all directions, with the fewest from the east (Figure 2.5). The total number of blowing snow events recorded over the range of the data was 4,514. Of those events, 962 of them were classified as severe. The wind directions involved in the severe events are displayed in Figure 2.6. The directions most common for severe blowing snow events in Winnipeg are with winds from the northwest, or the south.

Saskatoon, located farther north in the prairie eco-climatic zone, received a lower number of blowing snow events than Winnipeg. Wind events for this location appear to be spread almost evenly around the compass (Figure 2.7). The total number of observed events was 2,499. Events which were regarded as severe totalled 277. Wind data for the most severe events is displayed in Figure 2.8. The most common directions for severe blowing snow for Saskatoon are from the southeast, the north, and northwest, with none of the most extreme events occurring with southeast winds.

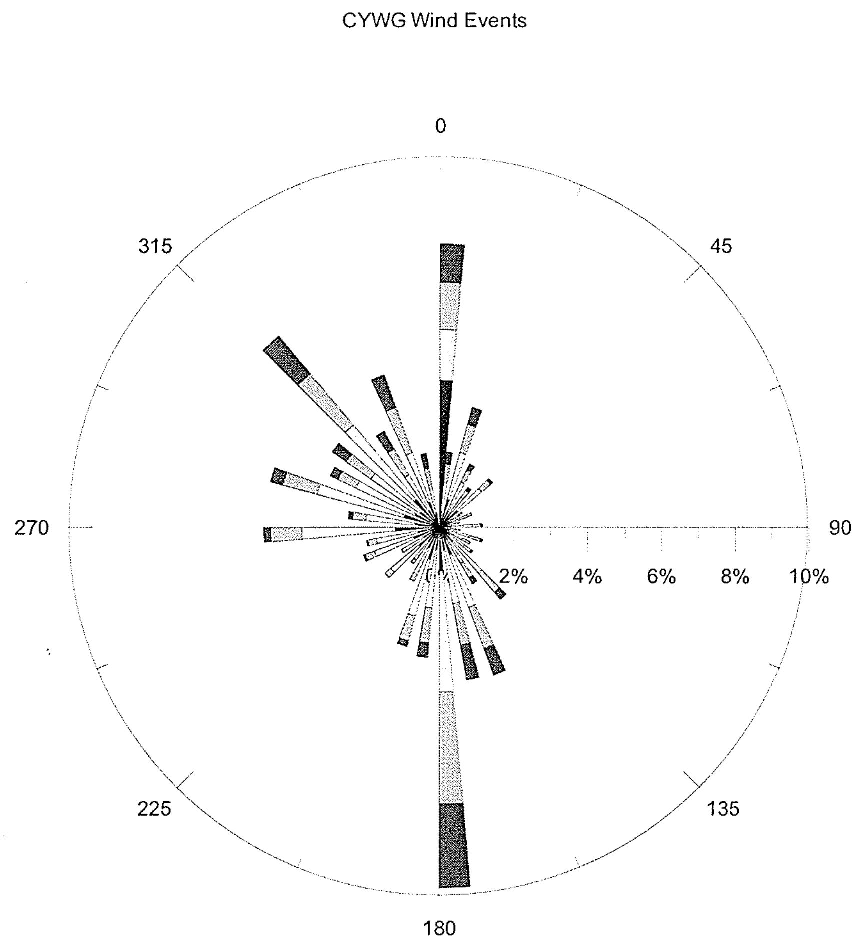

Figure 2.5 Complete wind rose for Winnipeg. Blue sections in the chart show wind speeds less than or equal to 10 km h^{-1}, yellow 10 to 20 km h^{-1}, green 20 to 30 km h^{-1}, and red greater than 30 km h^{-1}.

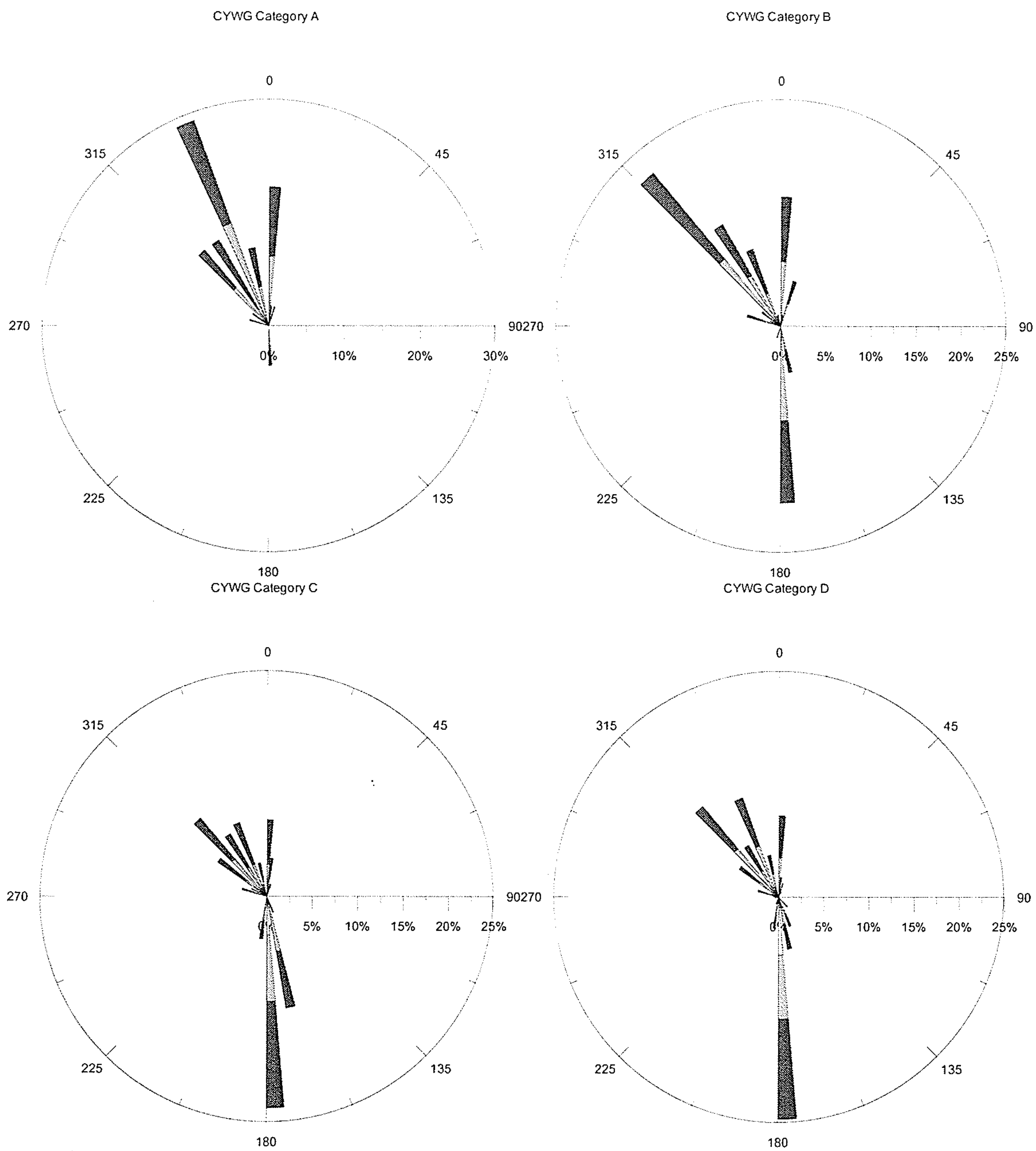

Figure 2.6 Wind roses for each category of severe blowing snow events for Winnipeg. Blue sections in the chart show wind speeds less than or equal to 10 km h^{-1}, yellow 10 to 20 km h^{-1}, green 20 to 30 km h^{-1}, and red greater than 30 km h^{-1}.

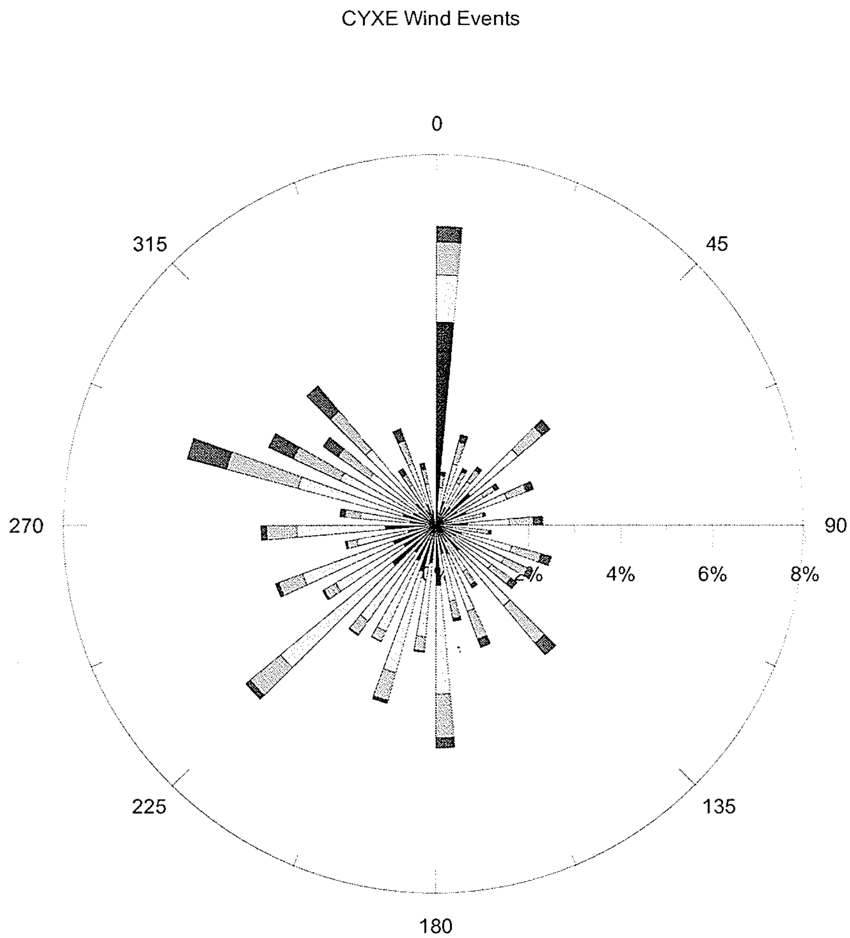

Figure 2.7 Complete wind rose for Saskatoon. Blue sections in the chart show wind speeds less than or equal to 10 km h^{-1}, yellow 10 to 20 km h^{-1}, green 20 to 30 km h^{-1}, and red greater than 30 km h^{-1}.

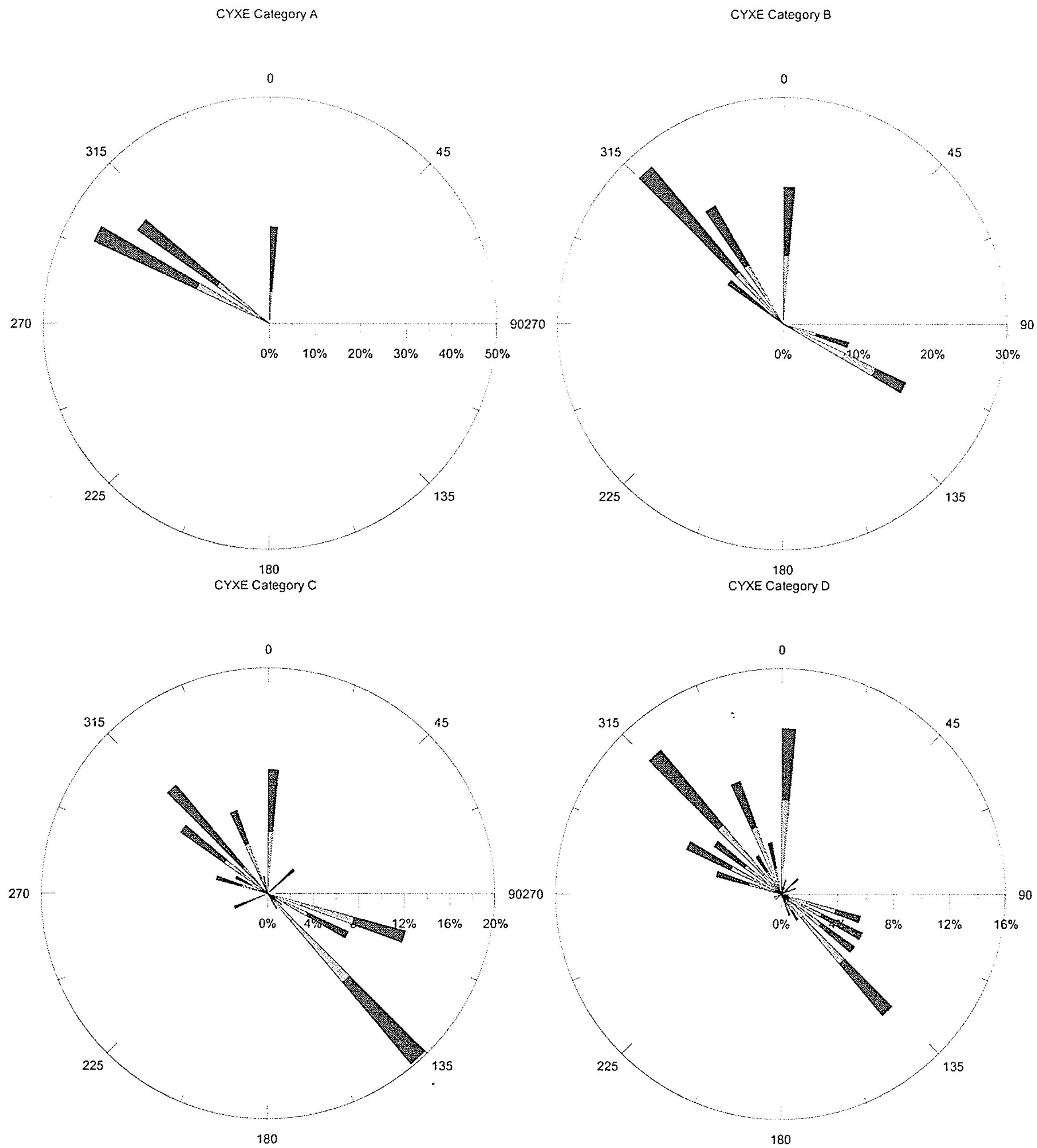

Figure 2.8 Wind roses for each category of severe blowing snow events for Saskatoon. Blue sections in the chart show wind speeds less than or equal to 10 km h^{-1}, yellow 10 to 20 km h^{-1}, green 20 to 30 km h^{-1}, and red greater than 30 km h^{-1}.

2.5 Forest Regions

Forest regions have a greatly decreased number of blowing snow events compared to the previous two regions. The two stations documented for this eco-climatic zone are Fort Smith and Fort Simpson. The predominant wind directions for Fort Simpson are north, north-northwest, and south, with the greatest number of events from the north (Figure 2.9). This could be due to the surrounding vegetation reducing the wind speed at the surface, preventing the threshold wind speed from being reached. The most severe events appear to come exclusively from the north-north west, with the most severe occurring with wind speeds below 20 km h^{-1}. These events may have occurred after recent snowfalls, accounting for the low wind speeds (Figure 2.10). Fort Simpson had a total of 1,120 blowing snow events, with 93 of these events regarded as severe. Fort Smith has the same pattern for wind as Fort Simpson Figure 2.11. Observers recorded 1181 blowing snow events, with 213 of them regarded as severe at this station. The direction of the severe blowing snow events was also quite similar to those observed at Fort Simpson although the primary direction at this location is northwest, not north-northwest (Figure 2.12).

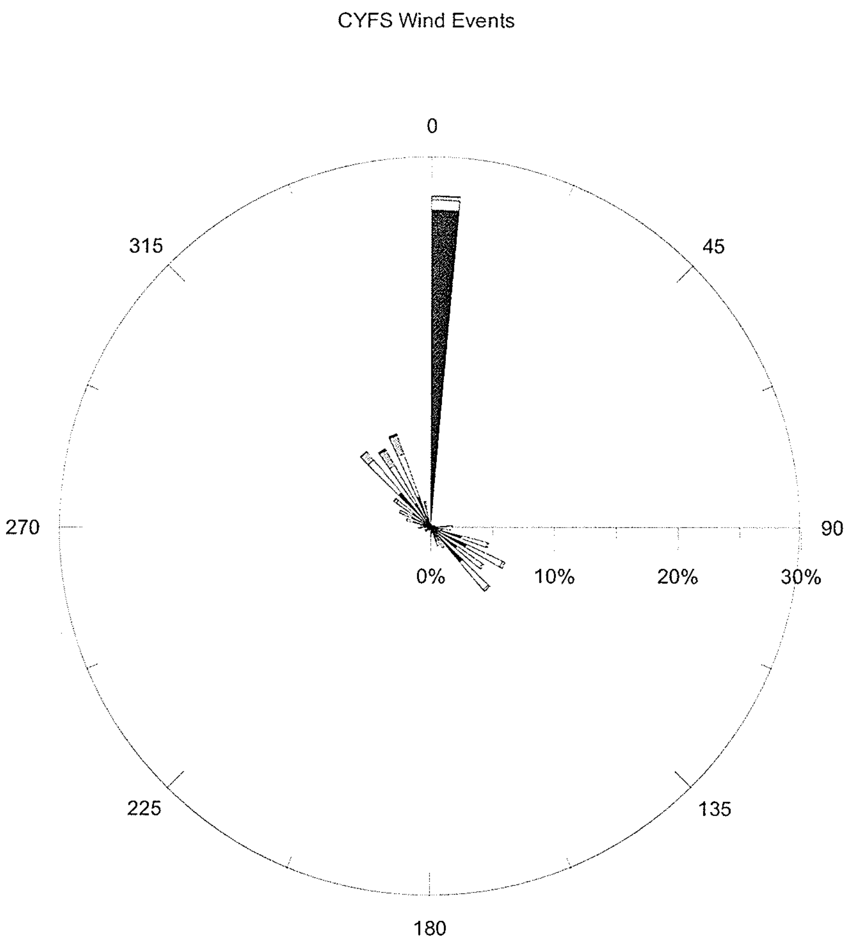

Figure 2.9 Complete wind rose for Fort Simpson. Blue sections in the chart show wind speeds less than or equal to 10 km h^{-1}, yellow 10 to 20 km h^{-1}, green 20 to 30 km h^{-1}, and red greater than 30 km h^{-1}.

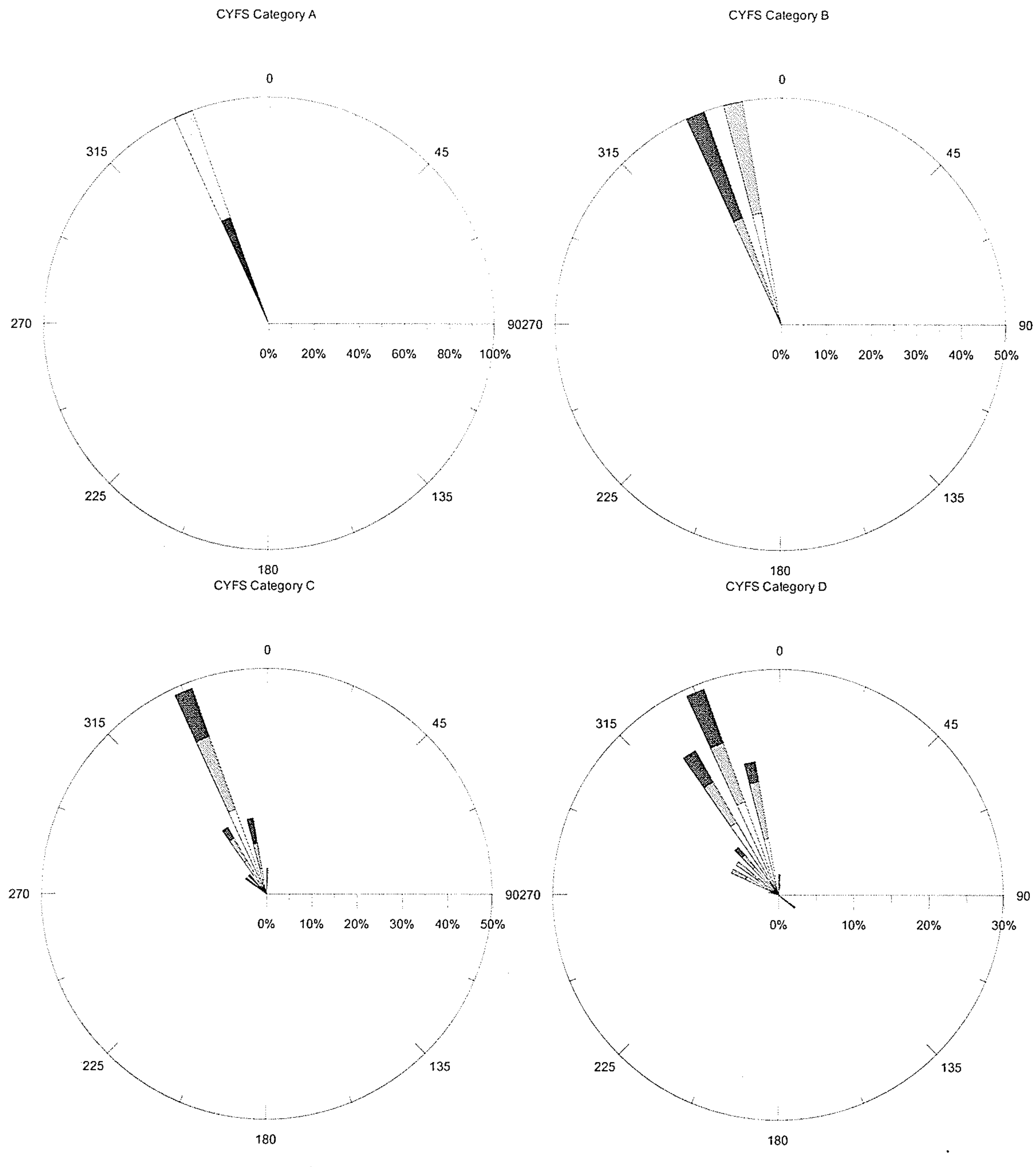

Figure 2.10 Wind roses for each category of severe blowing snow events for Fort Simpson. Blue sections in the chart show wind speeds less than or equal to 10 km h^{-1}*, yellow 10 to 20 km* h^{-1}*, green 20 to 30 km* h^{-1}*, and red greater than 30 km* h^{-1}*.*

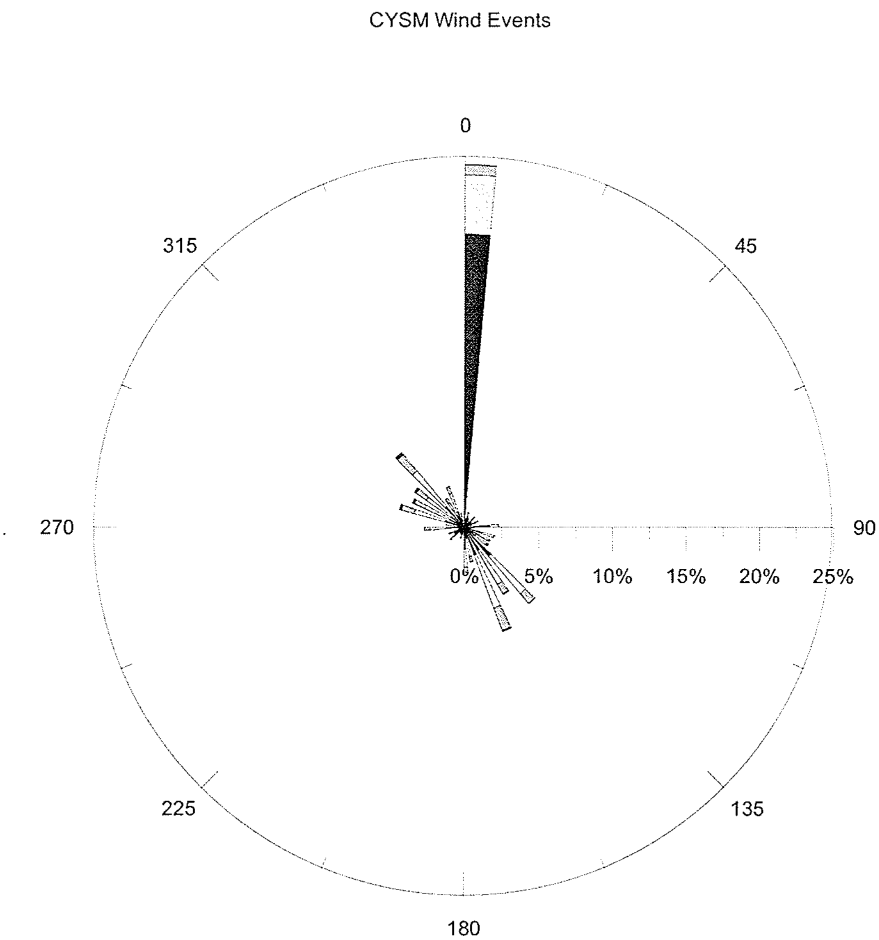

Figure 2.11 Complete wind rose for Fort Smith. Blue sections in the chart show wind speeds less than or equal to 10 km h^{-1}, yellow 10 to 20 km h^{-1}, green 20 to 30 km h^{-1}, and red greater than 30 km h^{-1}.

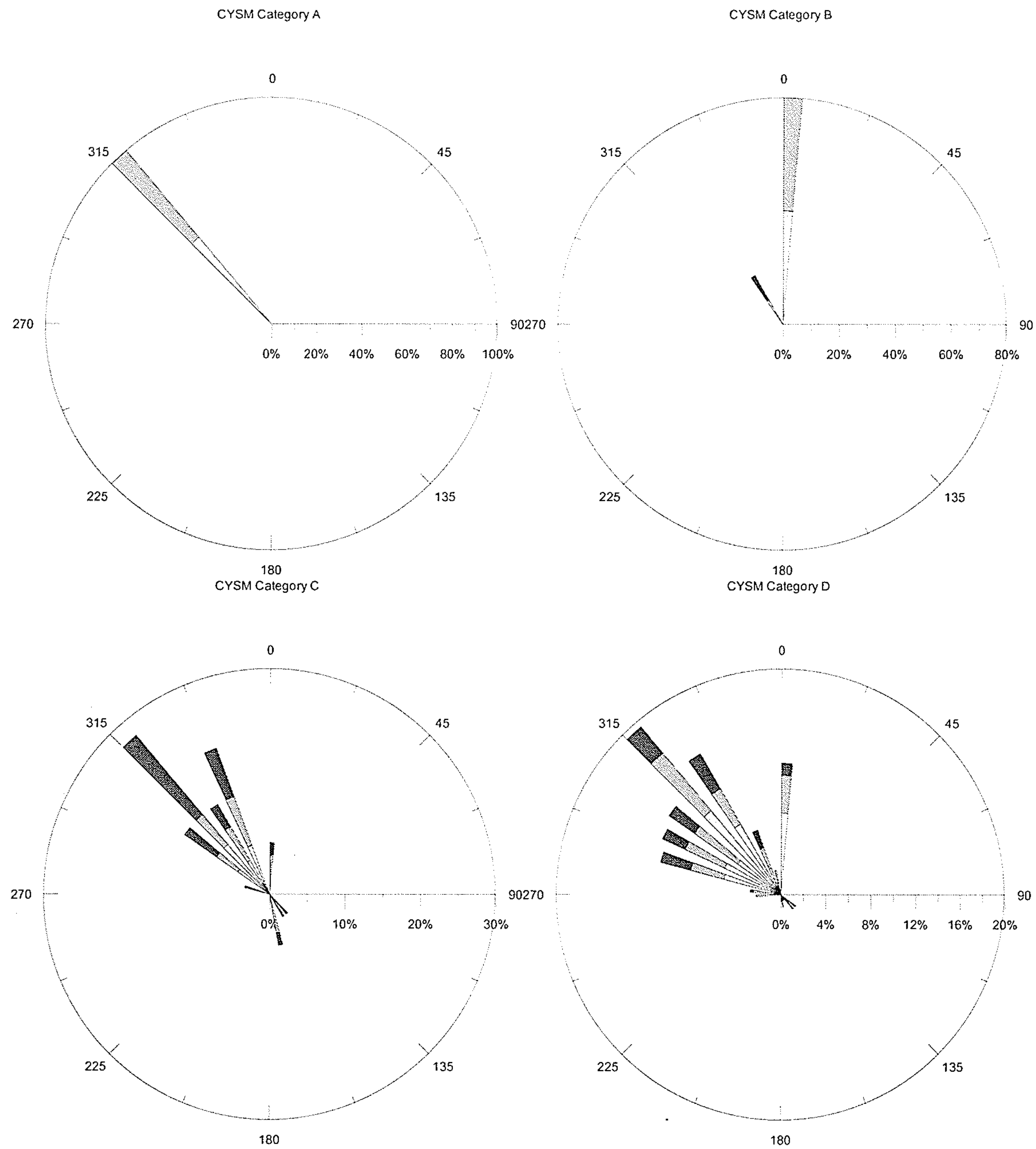

Figure 2.12 Wind roses for each category of severe blowing snow events for Fort Smith. Blue sections in the chart show wind speeds less than or equal to 10 km h^{-1}, yellow 10 to 20 km h^{-1}, green 20 to 30 km h^{-1}, and red greater than 30 km h^{-1}.

2.6 Mountain Regions

Mountain regions also have a lower number of blowing snow events than Prairie or Arctic regions. For this area, it is mainly due to topography. Edmonton, and the other three stations categorized as Mountain stations are not strictly within the Mountain eco-zone, but the weather is strongly influenced by the mountains, and therefore for the purpose of this thesis has been included in the Mountain eco-zone (John Hanesiak, personal communication). Edmonton has wind events from most directions, only it appears to lack many events from just east of north to straight east (Figure 2.13). The severest events for Edmonton come from wind from the north, and the severity appears to decrease as the winds shift towards the west (Figure 2.13). From the observations there were 863 blowing snow events, with 71 of those classified as severe. Wind events for Red Deer come mostly from the north and south (Figure 2.15). Data showed a total of 893 blowing snow events, with 73 of those severe. Like Edmonton, the most severe events occurred with north winds, and the severity diminished as the winds shifted towards the west (Figure 2.16).

CYEG Wind Events

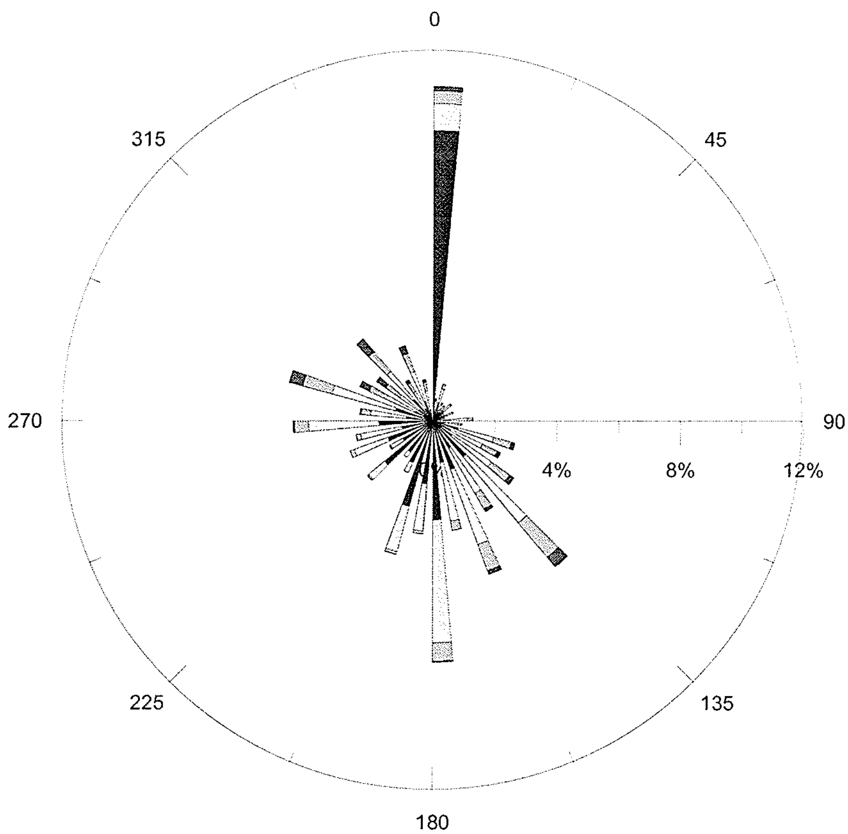

Figure 2.13 Complete wind rose for Edmonton. Blue sections in the chart show wind speeds less than or equal to 10 km h^{-1}, yellow 10 to 20 km h^{-1}, green 20 to 30 km h^{-1}, and red greater than 30 km h^{-1}.

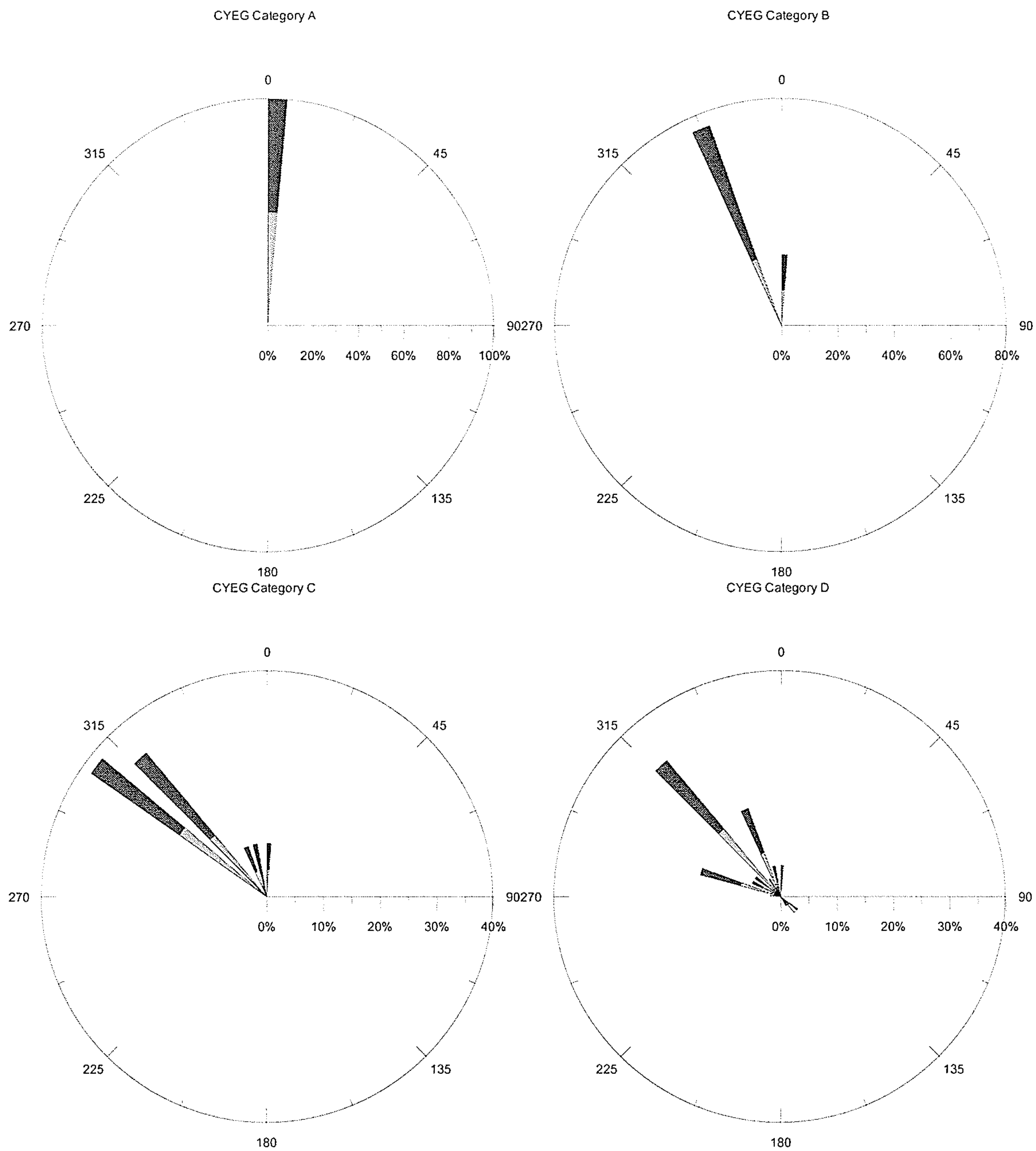

Figure 2.14 Wind roses for each category of severe blowing snow events for Edmonton. Blue sections in the chart show wind speeds less than or equal to 10 km h^{-1}, yellow 10 to 20 km h^{-1}, green 20 to 30 km h^{-1}, and red greater than 30 km h^{-1}.

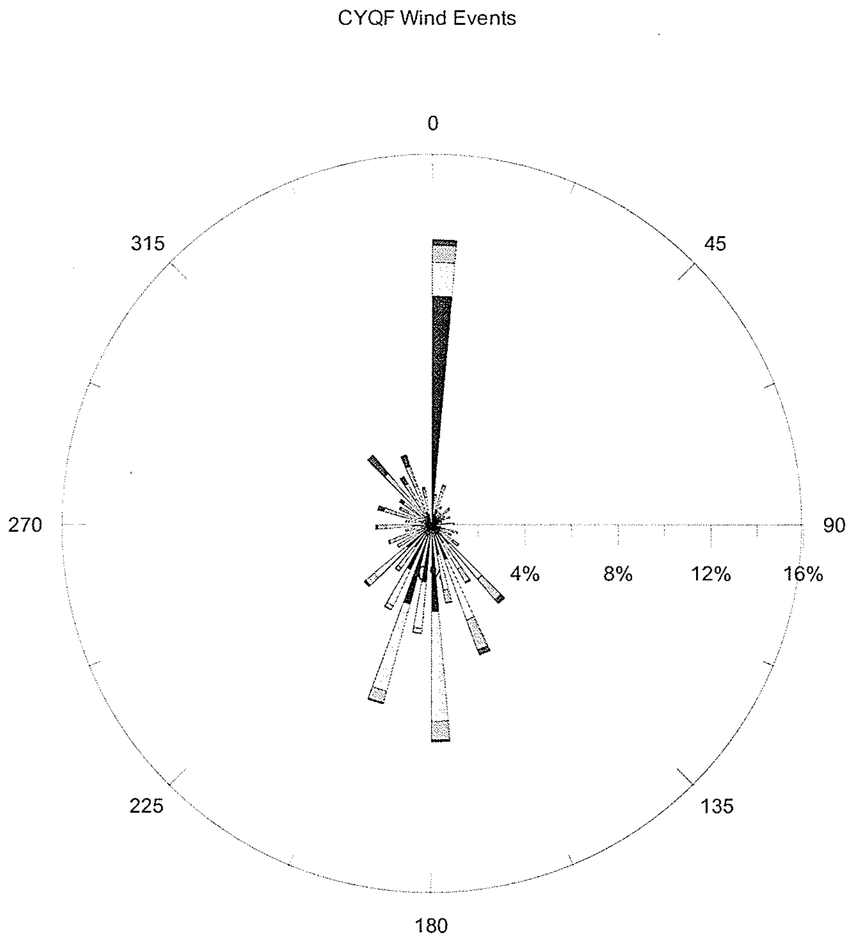

Figure 2.15 Complete wind rose for Red Deer. Blue sections in the chart show wind speeds less than or equal to 10 km h^{-1}, yellow 10 to 20 km h^{-1}, green 20 to 30 km h^{-1}, and red greater than 30 km h^{-1}.

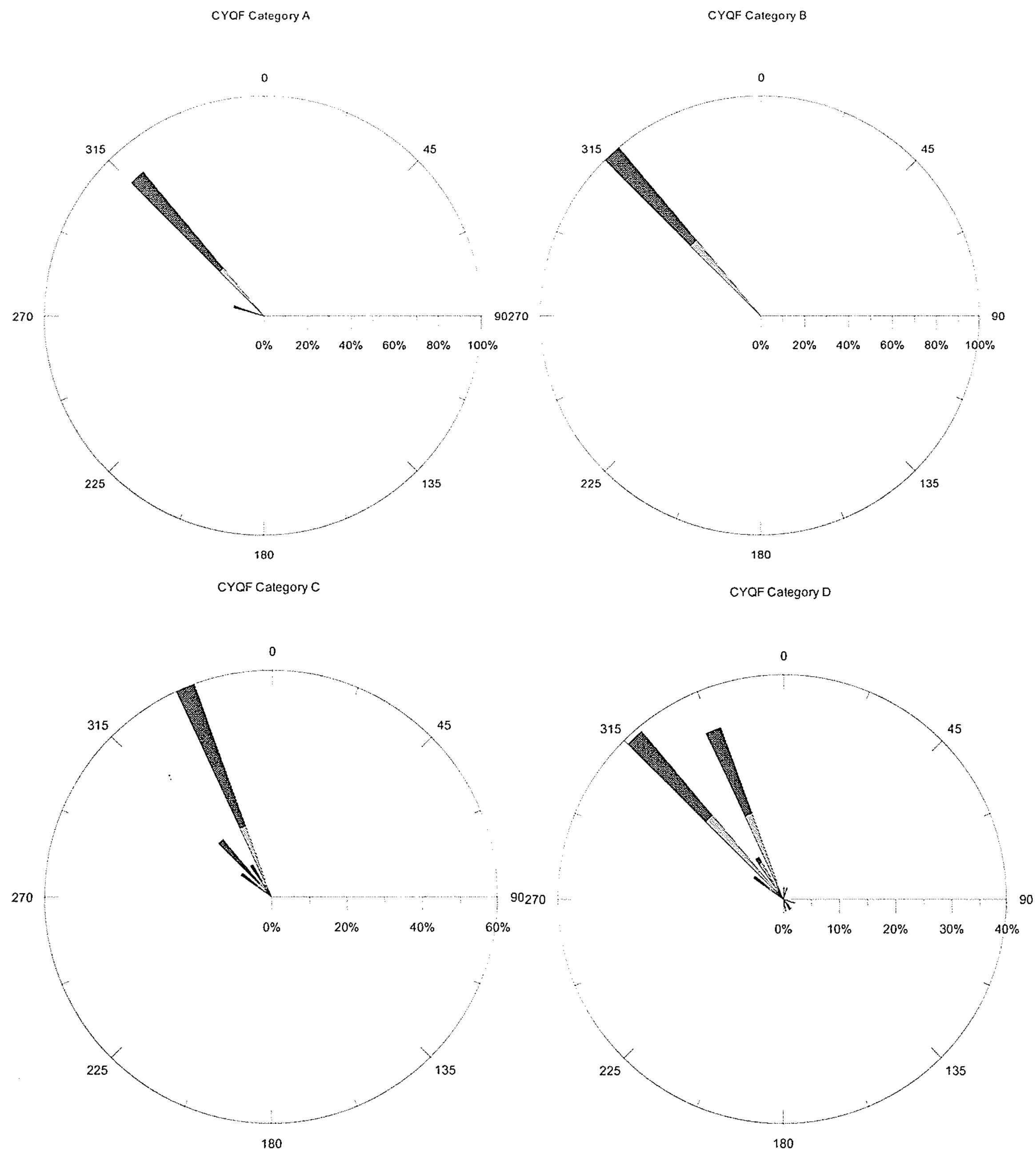

Figure 2.16 Wind roses for each category of severe blowing snow events for Red Deer. Blue sections in the chart show wind speeds less than or equal to 10 km h^{-1}, yellow 10 to 20 km h^{-1}, green 20 to 30 km h^{-1}, and red greater than 30 km h^{-1}.

2.7 Discussion

Of all the eco-climatic zones, the Arctic regions had the most blowing snow events because of their lack of major surface vegetation, and because of their longer season during which blowing snow can occur. The Prairie eco-climatic stations had the second highest number of blowing snow events. Like the Arctic region, interference from vegetation on a large scale had a negligible influence on blowing snow events.

Forest regions had very few blowing snow events when compared to the Prairie and Arctic eco-climatic zones. The major influence in this zone is the shielding of the snow surface from the surrounding forest. With very few severe events recorded, the events with the lowest visibility occurred with lower wind speeds, less than 20 km h^{-1}, than the other two zones. Most of these events likely occurred after a snowfall, when the threshold wind speed required would be less than at any other time.

The Mountain eco-climatic zone showed the lowest number of severe events of all four eco-climatic zones. Part of this may be due to the topography influencing wind strength, with most of the wind events recorded being below 20 km h^{-1}. Another possible reason for low numbers of blowing snow events could be because of Chinooks occurring during the blowing snow season. These could either melt the surface of the snow, creating a covering of ice to prevent blowing snow events from occurring, or it could melt remaining snow, ending the blowing snow season.

In almost every case, the most severe blowing snow events were not caused by winds from the predominant wind direction. This could be a result of terrain or vegetation hindering blowing snow from the predominant wind direction, but it is unclear from the data available.

3: The PIEKTUK Blowing Snow Model

3.1 History

The original PIEKTUK model was developed by Déry et al (1998). Two versions were developed, a fetch dependant model (PIEKTUK-F) and a time dependant model (PIEKTUK-T) (Déry et al, 1998). Unlike other previous models, such as the Prairie Blowing Snow Model (PBMS), the PIEKTUK model takes into account the thermodynamic effects of the sublimation of blowing snow particles. Feedback from this process affects temperature, relative humidity, and particle size, which are all elements used in the calculations performed by the model. During blowing snow, air temperature is slightly decreased because energy is required to sublimate a portion of the particles. Relative humidity is increased by the water vapour produced from the sublimation of the particles, and the overall particle size is decreased by the sublimation of a part of their mass.

The next development of the PIEKTUK model was the creation of a bulk version (PIEKTUK-B) which greatly decreased the computational requirements of the model, thereby decreasing the runtime of the model (Déry and Yau, 1999). Although faster, the predictions of the size distribution of particles, and the total number of particles appeared less realistic than previous models (Déry and Yau, 2001b). The final evolution of the PIEKTUK model came with the creation of the double-movement version (PIEKTUK-D). This version of the model combined the speed of PIEKTUK-B with the particle distribution and size of the original spectral version. The version of the model used in this thesis was the PIEKTUK-B version. There have been previous analyses of the accuracy of the model before, but they all focused on the sublimation and transport calculations of the model. None of the previous studies attempted to find the accuracy of the visibility predictions of the model.

3.2 Model Inputs and Outputs

The PIEKTUK model requires a series of six inputs to complete the necessary calculations. First it requires a date and time for which to calculate a prediction. The next requirement is the 10 m wind speed, followed by the threshold for transport. If the threshold wind speed is not available, then repeating the 10 m wind speed is acceptable, provided the line including the calculations for the threshold have not been commented out in the model. The final inputs in sequence are the temperature, relative humidity, and air pressure. The relative humidity and air pressure are used by the model to calculate total transport and sublimation, and are not used in the visibility calculation preformed by the model. Each line of input data for the model is used for one visibility calculation. Previous visibility calculations have no effect on any future calculations.

One main question involved in this thesis looks at the calculation of the threshold wind speed (U10t) needed for blowing snow. The model calculates this by means of the equation

$$U10t = 9.43+0.18*Ti+0.0033*Ti^2 \tag{3.1}$$

where Ti is the temperature in degrees Celsius. The other questions in this thesis relate to the visibility predictions made by the model. The equation used for visibility is:

$$vis = min(3.912/(6.0*pi*Qext*beta^2*n(9)), 25000) \quad (3.2)$$

where Qext is the extinction efficiency, which is the ratio between radiation absorbed by a particle to the amount of radiation which intercepts the particle surface (Pomeroy and Male, 1988). Beta is the scale parameter of gamma distribution (m) (Déry , 2004), and n(9) is the height at which the model will calculate the visibility, in this case 2.5m. The level n(9) was selected because it was the default level for the model when it was received, and a large part of the analysis was completed before it was realized that it could have been changed to n(8), changing the observation height to 1.66m. The difference in the results from both analyses for a single station, CYBK was calculated, and the percent chance that the two proportions were the same was calculated by a two-sample difference of

Table 3.1 The chance that the difference in the results from the different prediction heights of the model are statistically equal

Model Version (Constant Modifier)	Chance Statistically Equal
-5	0.00%
-4	11.36%
-3	17.10%
-2	54.18%
-1	41.80%
0	62.42%
+1	82.58%
+2	83.36%
+3	100.00%
+4	92.82%
+5	100.00%
+6	85.72%

proportion test. While the lower values for the constant in the threshold wind speed equation versions of the model had a high chance of being statistically different, versions that had a higher constant value in the equation had a good chance of being statistically equal (Table 3.1). Because of this, the rest of the analysis was completed at the n(9) visibility level. The outputs of the model are separated into four different files. One file, called subl.dat contains the sublimation rate of blowing snow. The file tran.dat, contains the transport rate of blowing snow. Total.dat contains the totals for sublimation and transport. Finally, a file called all_output.dat contains the date, time, visibility, transport and sublimation information.

3.3 Data

The data used for this thesis was provided by Environment Canada. The data set consisted of hourly weather observations from October to April for 35 stations spread across the Prairies and the Arctic, (Table 3.2, Figure 3.1). The visibility observations were made following protocols from the MANOBS manual. Reductions in visibility were recorded when there was an obstruction to normal visibility. The MANOBS (1990) manual defines an obstruction to vision as "A meteor, other than precipitation, which reduces the horizontal visibility at eye level. Obstructions may be suspended in the atmosphere e.g., fog or haze, or blown from the earth's surface, e.g. blowing snow or blowing sand" where eye level is 1.8m. When manual observations were made, it was the prevailing visibility that was recorded. The prevailing visibility is the maximum visibility common to half or more of the horizon circle (MANOBS, 1990). An example of this is shown in Figure 3.2. If the visibility appears to fluctuate rapidly by a 1/4 statute mile (SM) or more, the visibility is considered to be variable, and the average of the observed value is considered the prevailing visibility and it is noted that the observation was variable (MANOBS, 1990). Each line of data included all of the necessary variables to run the PIEKTUK model, along with day and night visibility observations, information on precipitation, and the wind direction. The start dates for individual data sets range from October 1960 to October 1978, and all of the data sets ended in March (Table 3.2). Four of the data sets, CYPG for example, have no observations past 1991. A portion of the wind speeds were recorded at heights other than the standard 10m, and they were transformed to 10 m by David Baggaley at Environment Canada. Some of the earliest data contained observations which were only recorded every three

Table 3.2 Station names, abbreviations, data start and end dates, and lines of data.

Station Name	Abbreviation	Start of Observations (October of year)	End of Observations (March of year)	Number of Lines of Data
Baker Lake	CYBK	1960	2001	163154
Brandon	CYBR	1960	2001	176883
Cambridge Bay	CYCB	1960	2001	169474
Kugluktuk	CYCO	1978 (Jan)	2001	91966
Dauphin	CYDN	1960	1991	134986
Edmonton	CYEG	1961 (Jan)	2001	176707
Estevan	CYEN	1960	2001	178904
Inuvik	CYEV	1960	2001	169417
Iqualuit	CYFB	1960	2001	170156
Fort Simpson	CYFS	1963 (Nov)	2001	156099
Hay River	CYHY	1960	2001	169887
Pond Inlet	CYIO	1975	2001	102513
Moose Jaw	CYMJ	1960	1991	135326
Prince Albert	CYPA	1960	2001	178464
Peace River	CYPE	1960	1991	134560
Portage	CYPG	1960	1991	134781
Red Deer	CYQF	1960	2001	178476
Regina	CYQR	1960	2001	178879
Yorkton	CYQV	1960	2001	178539
North Battleford	CYQW	1960	2001	178391
Resolute	CYRB	1960	2001	163466
Fort Smith	CYSM	1960	2001	165039
Cape Dorset	CYTE	1970	2001	85435
Hall Beach	CYUX	1960	2001	170007
La Ronge	CYVC	1960	2001	142533
Norman Wells	CYVQ	1960	2001	169761
Winnipeg	CYWG	1960	2001	177339
Saskatoon	CYXE	1960	2001	177312
Medicine Hat	CYXH	1960	2001	178434
Whitehorse	CYXY	1960	2001	126551
Calgary	CYYC	1960	2001	178949
Swift Current	CYYN	1960	2001	169582
Churchill	CYYQ	1960	2001	173946
Yellow Knife	CYZF	1960	2001	196523
Coral Harbour	CYZS	1960	2001	168223
			Total Lines of Data	5600662

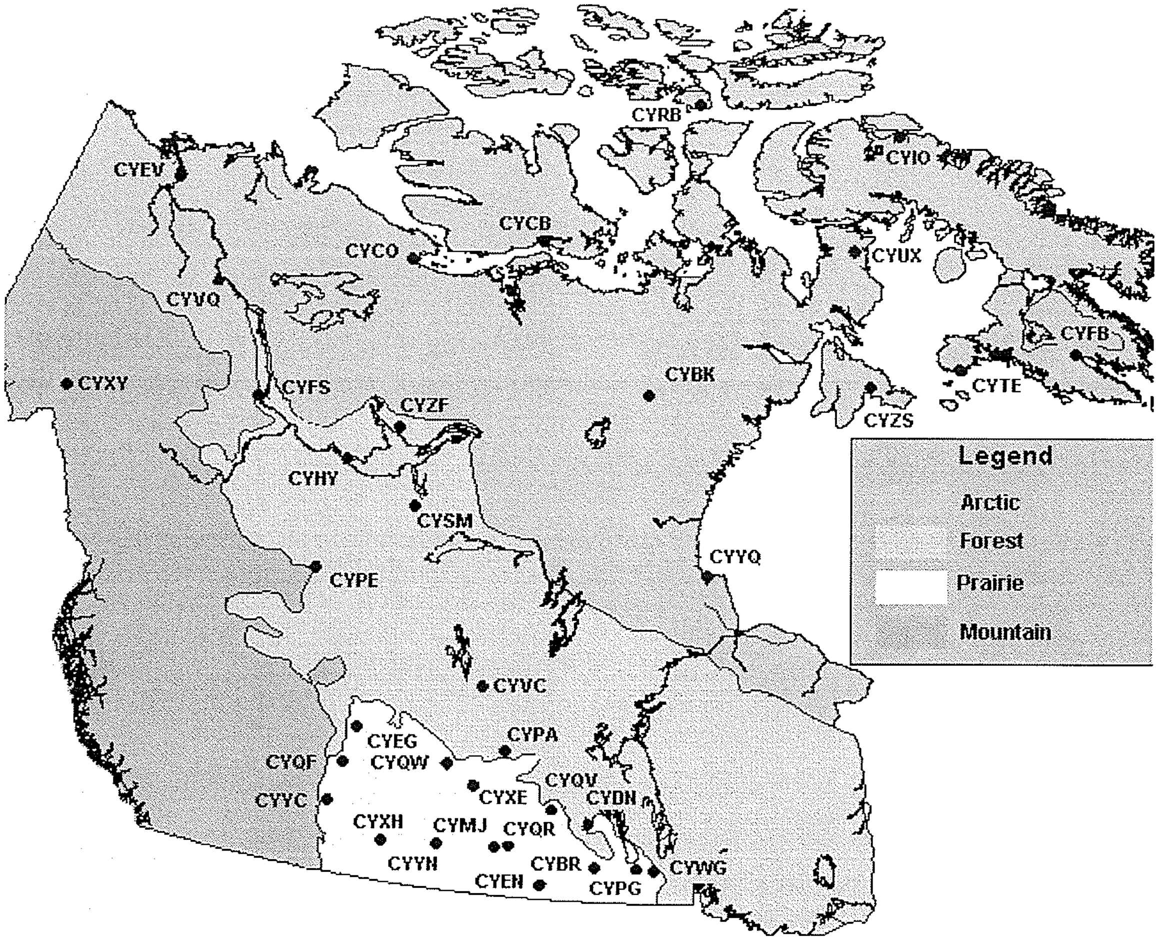

Figure 3.1 A map of all weather observation stations for which data was used and the eco-climatic zones throughout the region.

hours. Filling in the missing lines were null lines of text which needed to be stripped out and extraneous variables removed before the data could be used. This was accomplished by the use of a C++ program which was designed for this purpose.

EXAMPLE I

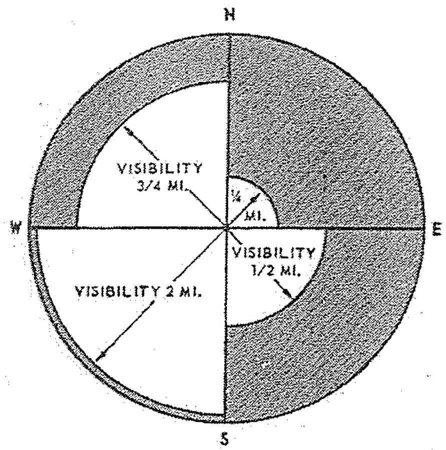

EXAMPLE II

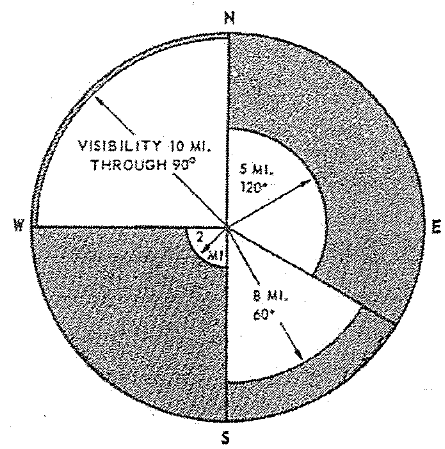

Note: Point of observation is centre of circle

PREVAILING VISIBILITY = 3/4 mi.

Notes:
(i) The prevailing visibility is not 2 miles because 2 miles is common to only 90° of the horizon circle.

(ii) 3/4 of a mile is considered to be the prevailing visibility because this is the greatest value common to 1/2 or more (180°) of the horizon circle.

PREVAILING VISIBILITY = 5 mi.

Notes:
(i) The prevailing visibility is not 10 miles because 10 miles is common to only 90° of the horizon circle.

(ii) The prevailing visibility is not 8 miles because 8 miles is common to only 150° of the horizon circle (90° + 60°).

(iii) The prevailing visibility is considered to be 5 miles because this is the maximum value common to 1/2 or more of the horizon circle, i.e., 90° + 60° + 120° .

Figure 3.2 An example of how visibility observations are calculated from the MANOBS (1990) manual.

4: The Accuracy of the PIEKTUK Blowing Snow Model

4.1 Introduction

In this chapter I test the accuracy of the PIEKTUK Blowing Snow Model for its detection of blowing snow, and its visibility estimates against meteorological station data. For forecasting purposes, it is imperative that the models used are as accurate as possible. Any missed predictions could endanger lives, and false predictions could lead to people ignoring later predictions. The main questions addressed in this chapter are:

1) Does PIEKTUK accurately predict the occurrence of blowing snow?
2) Does the accuracy of the model vary over different eco-climatic zones?
3) How accurate are the visibility predictions in PIEKTUK?

4.2 Prediction of the Occurrence of Blowing Snow

4.2.1 Methods

The PIEKTUK model obtains its threshold wind speed from Equation 3.1 (Page 28). The model uses this equation as a Boolean variable to determine whether blowing is occurring or not. Once this has been determined, the model either goes on to make a prediction of the visibility, or it returns to obtain another line of data.

The data was run through the model and the four output files were combined with the input files, to create one large file containing each unique observation on the same line as its corresponding model output. These combination files were then analyzed by another C++ program which counted the number of times the model was correct (X), either by predicting blowing snow when an observation of blowing snow was present or by predicting no event when none occurred. The program also counted the number of times the model over-predicted (Z) by indicating an event when none was recorded in the observations, and the number of under-predictions (Y), when the model missed an event present in the observations (Table 4.1).

Table 4.1 Model hits and misses (over- and under-prediction).

Blowing Snow	Observed	Predicted	Not Observed	Not Predicted
X	√	√	√	√
X2	√	√		
Y	√			
Z		√		

Using these numbers, the probability of detection (POD), the false alarm ratio (FAR), and the CSI, the accuracy of the model was evaluated. These numbers were calculated as follows:

$$POD = X/(X+Y) \qquad (4.1)$$

$$FAR = Z/(X+Z) \qquad (4.2)$$

$$CSI(X) = X/(X+Y+Z) \qquad (4.3)$$

The model was also evaluated without counting null weather events, days when blowing snow was neither predicted nor observed. The only events that were counted as correct predictions were those that actually had blowing snow occurring along with a prediction of the event (X2). Each of the three previous calculations was repeated using X2 in the place of X, while Y and Z remained the same. These calculations were performed for each station, and also for the individual eco-climatic zones. The calculation for the eco-climatic zones used the totals of the X, X2, Y and Z values from each station and then the calculations for POD, FAR, and CSI. Another calculation for overall results was completed using the same method as for the eco-climatic zones. The CSI method of analyzing results was also used by Baggaley and Hanesiak (2005)in their analysis.

4.2.2 Results

Including null weather events, the PIEKTUK model performed well with all eco-climatic zones combined, with the probability of detection reaching 99.80%, and a FAR of only 7.10%. The critical success index X values was 93.76% for all sites (Figure 4.1).

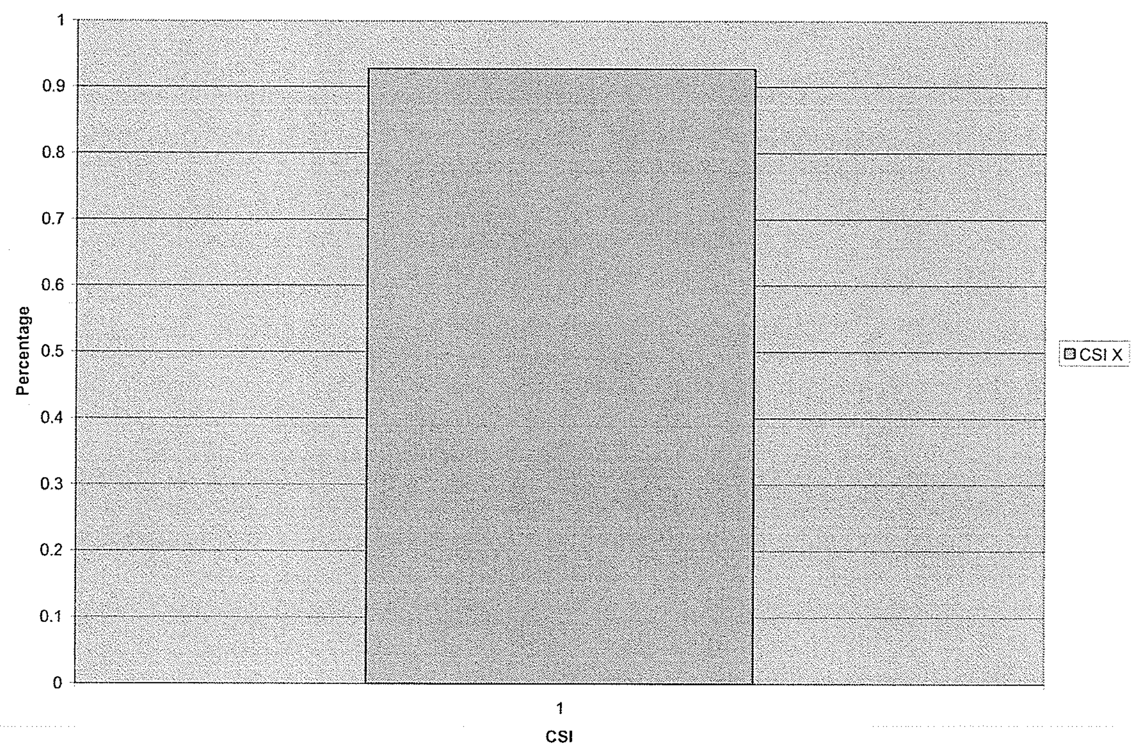

Figure 4.1 The overall performance of the PIEKTUK model.

Once the null weather events were removed, the results were not as promising for the predictive capabilities of the PIEKTUK model. The probability of detection (POD) still remained high, but decreased slightly, to a value of 93.02%. The probability of an over-prediction of an event (FAR) increased dramatically to 74.52%. The critical success index (CSI) also had a large change from its previous value to 25.00%. A detailed breakdown by station is presented in Appendix A.

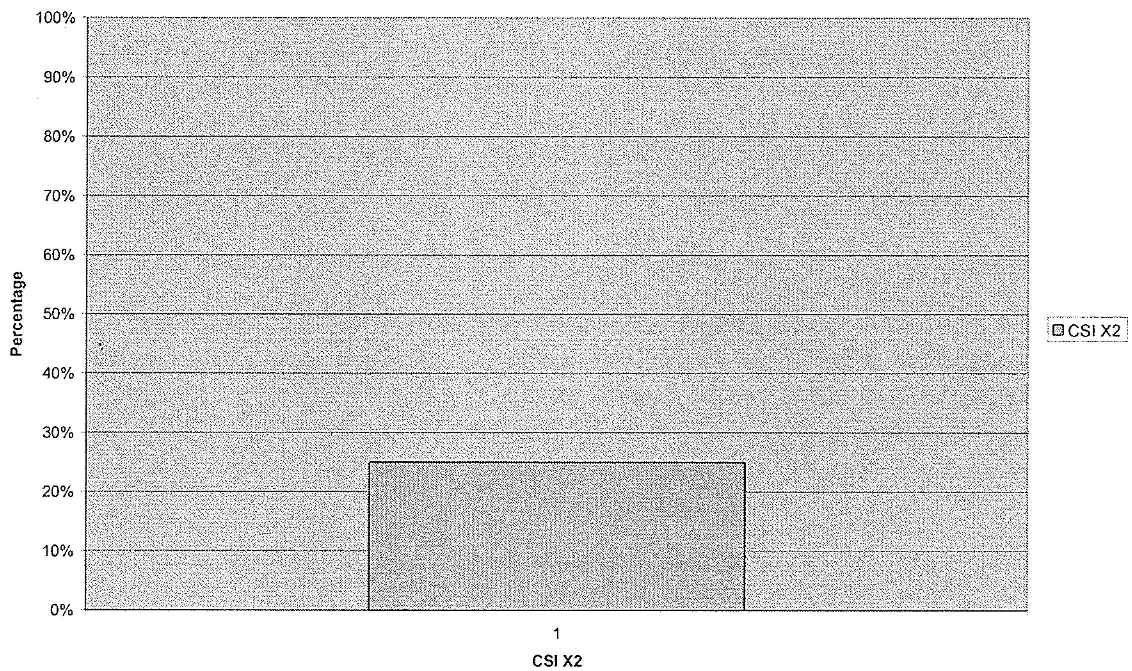

Figure 4.2 Overall performance of the PIEKTUK model with null weather events removed.

4.2.3 Conclusions

From the results, there is definite room for improvement in the model. It performed well overall, but when null weather conditions were excluded, the change in performance was dramatic. The total number of correct predictions for the model goes from a total of 3,227,811 (X) to 83,961 (X2), while both over predictions and under predictions remain steady at their previous values. The model has a tendency to over-predict the occurrence of blowing snow events. This could be due to the calculation of the threshold wind speed being too low, thereby allowing the model to forecast blowing snow when none was actually present. The values predicted by the model are far below the results of Baggaley and Hanesiak (2005) of a CSI value of 66% with their empirical forecasting method.

4.3 Eco-climatic Zone Analysis

4.3.1 Methods

To find out how the model preformed over the different eco-climatic zones, the stations were broken down into Arctic, Prairie, Mountain, and Forest categories, and the same analysis as that was preformed at the beginning of this chapter was preformed again. The analysis was repeated a second time with null weather events excluded, and the number of correct predictions, over-predictions and under-predictions totalled, and the POD, FAR, and CSI calculated.

4.3.2 Results

With null weather events included, the POD for all eco-climatic zones was close to 100%. FAR were all below 7%, with the exception of the Arctic zone which had a FAR of 18.90%. Prairie, Forest, and Mountain zones had CSI vales above 93%, while once again the Arctic zone had the lowest value of 79.01% (Table 4.2). Once the null values were removed from the analysis, there was a drop of 15% to 20% in the POD for all regions, and a huge increase in the FAR. The CSI dropped drastically across all eco-climatic regions (Table 4.3).

Table 4.2 Values from initial analysis including null weather events by eco-climatic zone (X).

Eco-climatic Zone	X	Y	Z	POD	FAR	CSI
Arctic	527648	16581	122953	96.95%	18.90%	79.09%
Prairie	1079399	916	77701	99.92%	6.72%	93.21%
Forest	1093804	721	35764	99.93%	3.17%	96.77%
Mountain	526960	50	9104	99.99%	1.70%	98.29%

Table 4.3 Values from initial analysis excluding null weather events by eco-climatic zone (X2).

Eco-climatic Zone	X2	Y	Z	POD	FAR	CSI
Arctic	68624	16581	122953	80.54%	64.18%	32.97%
Prairie	11333	916	77701	92.52%	87.27%	12.60%
Forest	3587	721	35764	83.26%	90.88%	8.95%
Mountain	417	50	9104	89.29%	95.62%	4.36%

4.3.3 Conclusions

Even with drastic differences between the numbers of events recorded for each eco-climatic zone, the same pattern was observed. Initially, before the null weather events were excluded, the model performed very well. Once the null weather events were removed, a different story was revealed. As seen previously, even the results are broken down into eco-climatic zones, the results for just the Arctic stations are far below what Baggaley and Hanesiak (2005) calculated in their study. For the eco-climatic zones there was still a high POD, so very few blowing snow events were missed, but there was also a high FAR, which meant that there were a large number of incorrect predictions. The model performed the best in Arctic regions, and had extremely poor results in Mountain regions. The PIEKTUK model needs to have modifications made to reduce the number of over-predictions to increase the accuracy of the blowing snow forecasts for all regions. Once the number of over-predictions has been reduced, it may be possible to customize the model to perform better in each eco-climatic zone.

4.4 Visibility Testing

4.4.1 Methods

To test the accuracy of the visibility predictions of PIEKTUK, visibility thresholds were created. An accurate prediction occurred if both PIEKTUK and the actual observation were below the threshold (X), over-prediction if the model predicted below the threshold and the actual observations were above the threshold (Z), and under-prediction occurred if the observations were under the threshold while the model prediction was over the threshold visibility. Results are displayed by station by eco-climatic zone in Appendix B. The second method of evaluation was to discover how accurate the predictions of visibility were from the model when they were compared to actual visibility ranges. The same parameters as the previous analysis were used, with a correct prediction having both observed and predicted visibility within a range counting as correct (X), over-prediction if the model predicted a lower range than was actually observed (Z), and an under-prediction if the observed visibility was in a lower range than predicted by the model (Y). The visibility ranges are shown in Table 4.3 and a break down by station by eco-climatic zone is displayed in Appendix C.

Table 4.3 Maximum and minimum values for each of the visibility categories.

Range Label	Max Value	Min Value
9.6	10.4	8.8
8.0	8.8	7.2
6.4	7.5	5.6
4.8	5.6	4.0
3.2	4.0	2.4
1.6	2.0	1.2
0.8	1.0	0.6
0.4	0.6	0.2
0.2	0.2	0.0

4.4.2 Results

When the threshold visibilities were used to categorize the visibility predictions of the model into correct, over-, and under-predictions, the PIEKTUK model almost always over-predicted the reduction in visibility. The most accurate visibility threshold for predictions was 9.6 km, where the CSI X is 24.7% (Figure 4.3). The accuracy of the predictions for the visibility thresholds decreased as the range examined was decreased.

When the focus is strictly on visibility ranges, the performance of the model decreased even more. The most accurate visibility range for the model was 0.4 km, where the CSI X value was 5.3% (Figure 4.4). The model made very few correct predictions in the less essential categories, but when the predictions were made for severe reductions in visibility, 3 SM or less, the model made its most accurate predictions.

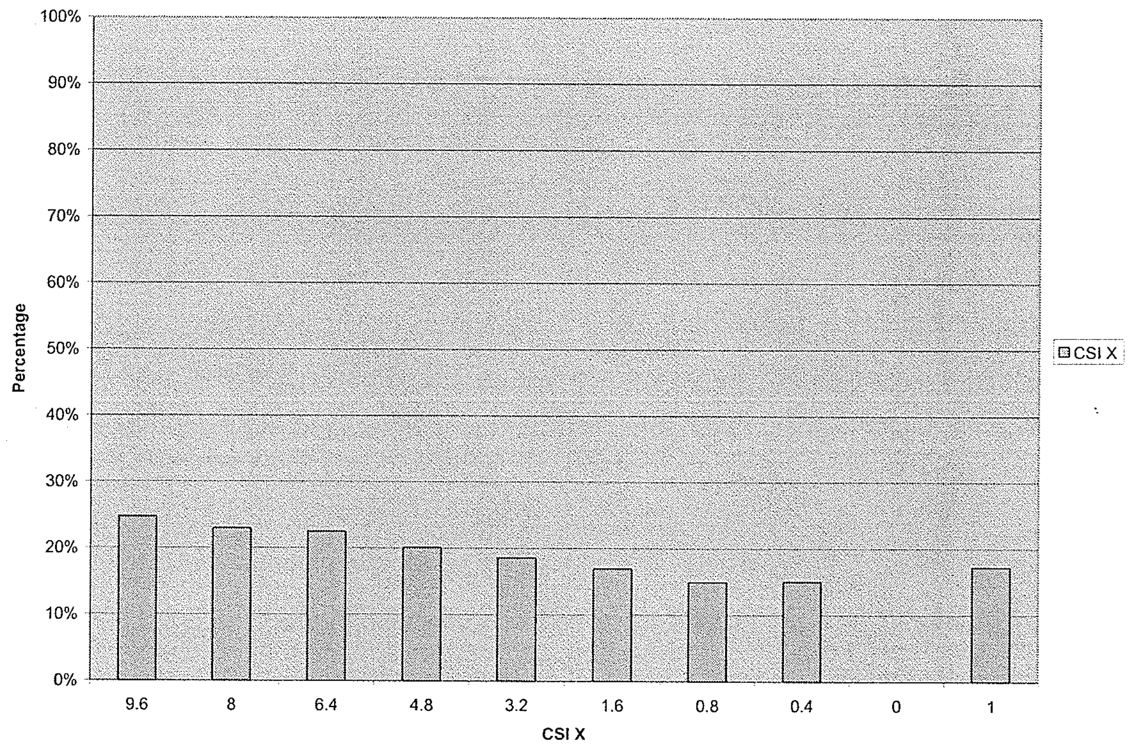

Figure 4.3 Analysis of the PIEKTUK model visibility predictions using visibility thresholds for all stations.

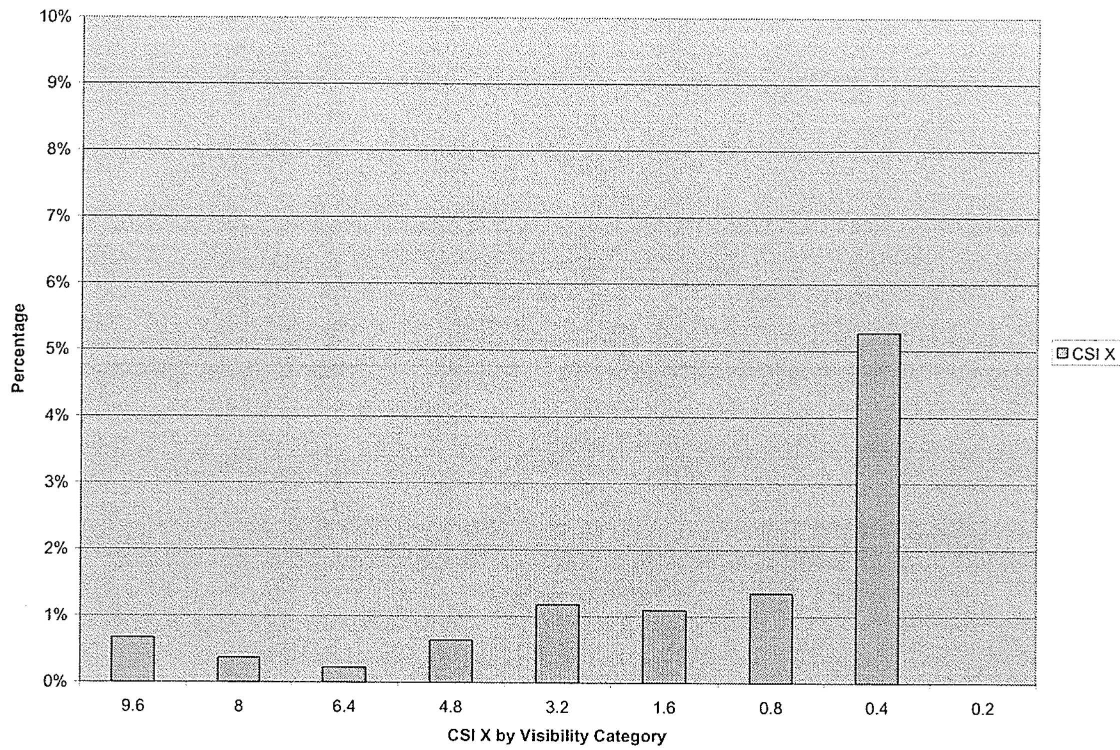

Figure 4.4 Analysis of visibility predictions by PIEKTUK using ranges of visibility for all stations.

4.4.3 Conclusions

From the analysis of visibility thresholds, the model will over-predict the reduction of the visibility approximately 75% of the time, and as the thresholds decrease the over-predictions move closer to 80%. The capability of the model to forecast visibility during a blowing snow event clearly needs to be improved.

When the focus is moved from visibility thresholds to visibility ranges, the performance of the model becomes even less reliable. With the highest critical success value of less than 6%, it is clearly impossible to rely on the current version of PIEKTUK to accurately predict visibility ranges during blowing snow events.

5: Modification of the PIEKTUK Blowing Snow Model

5.1 Introduction

The threshold wind speed was increased in increments of 1m s^{-1} to 6m s^{-1} above the current value, and also decreased by the same increment to 5m s^{-1} below the current value to find the optimum value of the threshold wind speed for specific stations for the model's predictive capability for visibility predictions. Also, data suggested that some stations never have blowing snow from certain directions, or only with very strong wind speeds. A modified dynamic version of PIEKTUK was created which allows for different threshold wind speeds from different directions. The main questions answered in this chapter are:

1) What is the optimum threshold wind speed for different regions and specific stations?
2) Does a dynamic model with different threshold wind speeds for different directions improve the visibility predictions?
3) Does the optimum threshold wind speed for a given direction change when analyzed at low visibility?

5.2 Optimum threshold wind speed

5.2.1 Methods

Once again the focus was the calculation of the threshold wind speed by the PIEKTUK model. The constant 9.43 was decreased by increments of 1 to 4.43 and increased by increments of 1 to 15.43, to create 11 "new" versions of the model.

$$U10t = 4.43 + 0.18 * T + 0.0033 * T2 \quad (5.1)$$

$$\uparrow$$

$$U10t = 9.43 + 0.18 * T + 0.0033 * T2$$

$$\downarrow$$

$$U10t = 15.43 + 0.18 * T + 0.0033 * T2$$

Each of these new models were run with the same data as the original version, creating a spectrum of results to show the influence of the threshold calculation, as well as the optimum value for each station and for each eco-climatic zone.

The same evaluation techniques were used in this stage of the analysis as were used in the previous section. The POD, FAR, CSI, and X versus X2 were calculated. These were then graphed in Excel side by side to determine which version of the model performed the best. The analysis was performed for a selection of stations across the eco-climatic zones because the length of time required by single station did not allow for the model runs to be performed for all stations.

5.2.2 Results

Using Baker Lake as an example, as the threshold wind speed was increased through the series of models, the number of hits (X2) decreased. The decrease was slow at first, but became more noticeable when the +1 version of the model was run. The number of under-predictions of the model (Y) slowly increased as the threshold wind speed was increased, while the opposite effect was seen in the over-predictions with a more pronounced decline (Figure 5.1)

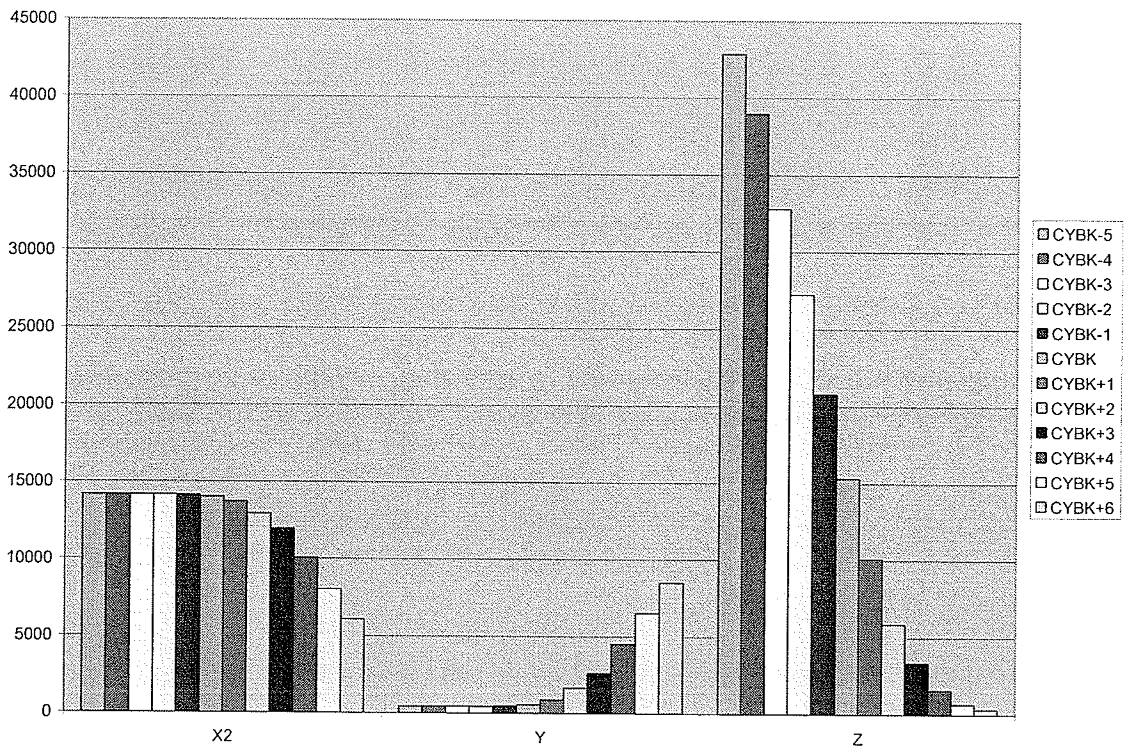

Figure 5.1 Counts for Baker Lake of X2, Y and Z for threshold testing.

Similar to the X2 values, the POD decreased as the threshold wind speed increased (Figure 5.2). The FAR response was similar to the drop in over-predictions. The CSI of X2 reached its highest value during the model run of the +3 version, 66.61% (Figure 5.2).

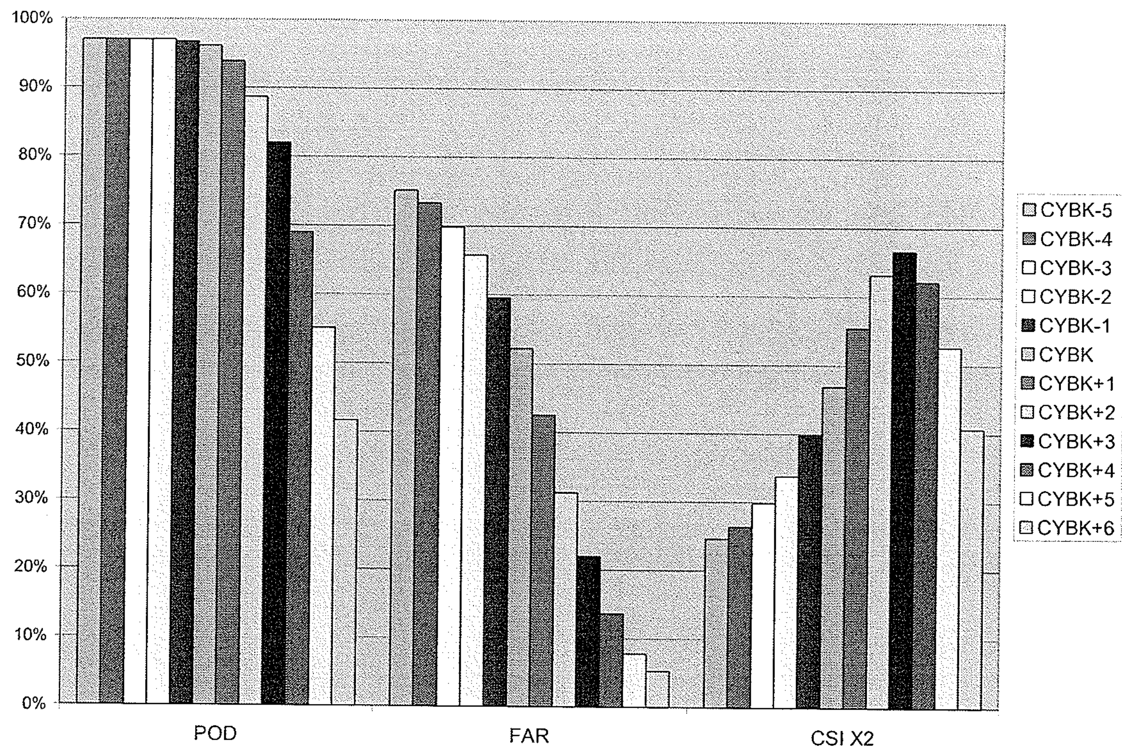

Figure 5.2 POD FAR and CSI of X2 for Baker Lake.

The results for Winnipeg mirrored the results of Baker Lake in the pattern of increases and decreases, and also the model run which produced the highest CSI X 2 value (Figures 5.3 and 5.4).

The optimum CSI X2 at other stations ranged from model run +1 (CYEV) to model run +5(CYDN). Arctic stations were very close in their optimum values, with the +3 model run being optimal. The optimal results for the Prairies were close to the same, with a little variance between +3 and +4. Stations in the Forest and Mountain areas had a larger variety in their optimum values (Table 5.1).

Some of the variability in the optimal version of the model between stations could be explained by terrain, vegetation, and elevation of surrounding terrain. An observation station which was elevated above the surrounding terrain could have a lower threshold

Table 5.1 Optimal model versions and their CSI(X2) value by station by eco-climatic zone.

Arctic	Optimal Model Version	CSI(X2)
CYZS	+3	60.99%
CYCB	+3	59.79%
CYCO	+3	42.94%
CYBK	+3	66.61%
CYYQ	+3	54.68%
CYFB	+2	44.77%
CYRB	+3	59.94%
Prairie		
CYXE	+3	28.33%
CYWG	+3	30.31%
CYEN	+4	26.62%
CYBR	+3	31.40%
CYQR	+4	36.64%
Forest		
CYDN	+5	36.97%
CYVQ	+2	35.70%
CYPE	+2	18.63%
CYSM	+2	18.37%
CYFS	+2	18.18%
CYEV	+1	28.66%
CYPA	+5	7.62%
Mountain		
CYQF	+4	18.61%
CYEG	+4	23.42%

wind speed than a station located in a valley. Other stations could have vegetation surrounding them which would hinder wind speeds at ground level, but would not register in the 10 m wind speed.

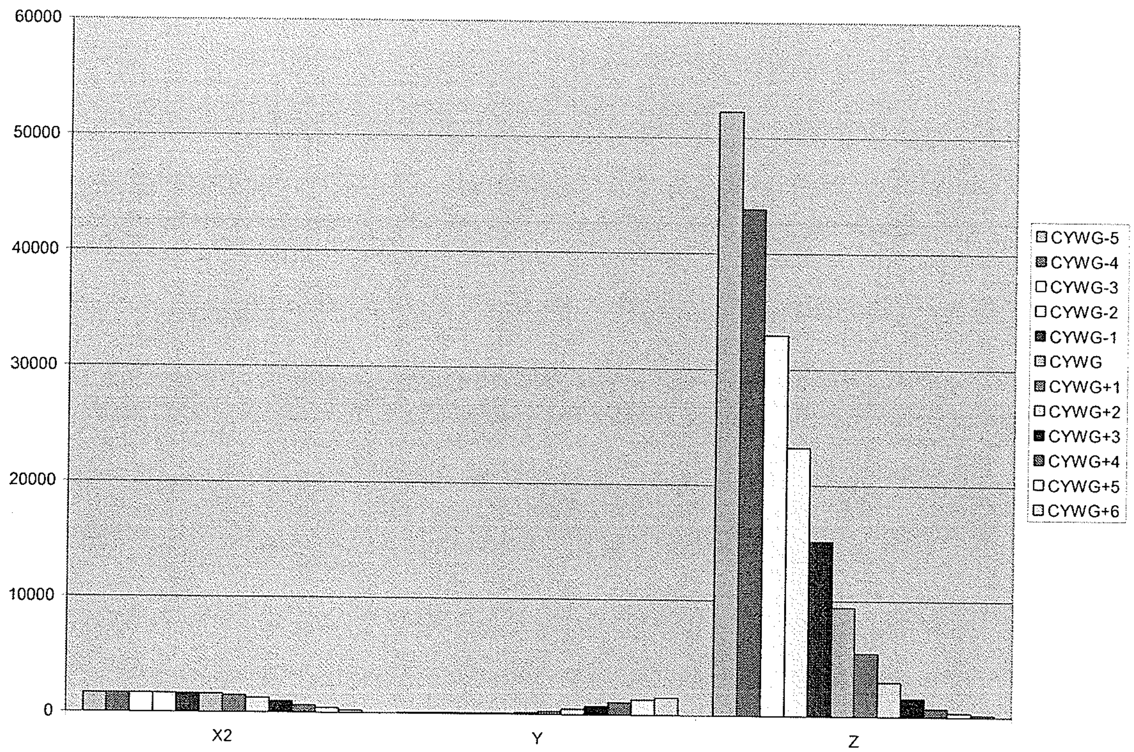

Figure 5.3 Threshold testing X2, Y and Z for Winnipeg

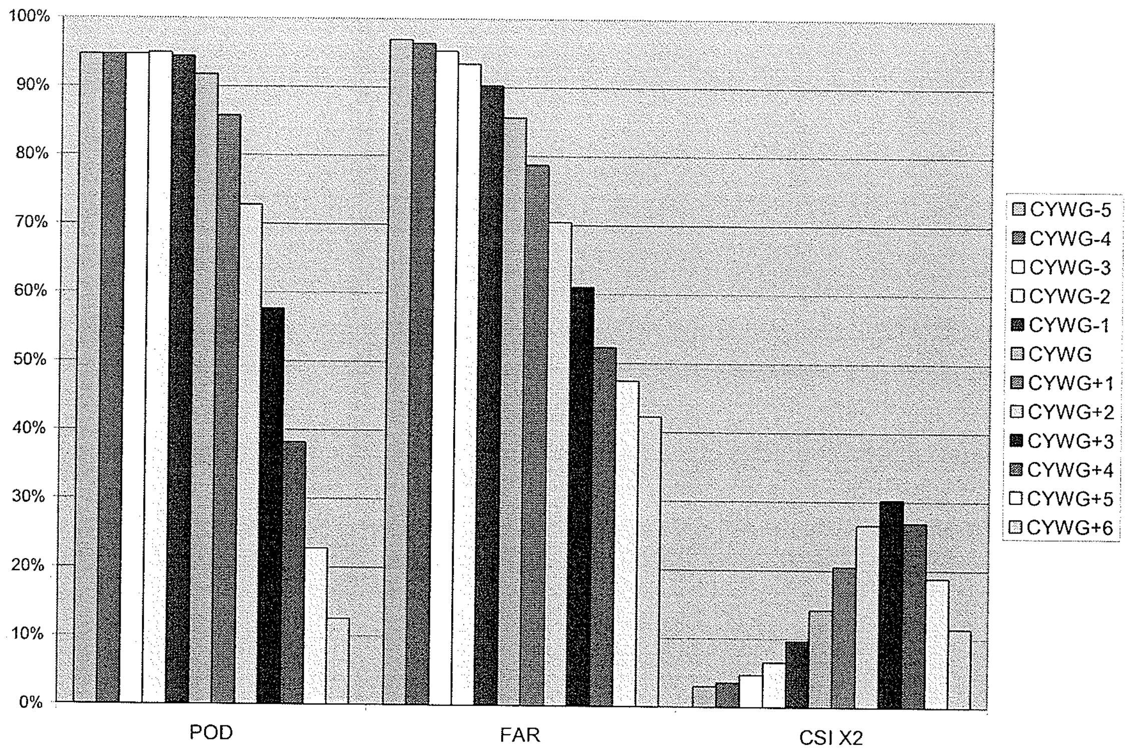

Figure 5.4 POD FAR and CSI of X2 of threshold testing for Winnipeg.

5.2.3 Conclusions

From the results, the version of the model which appears to be optimum for the most stations is +3. While the results range anywhere from +1 (CYEV) to +5 (CYEN), most of this variation is found in Mountain and Forest regions, probably due to the heterogeneous surrounding terrain and vegetation. Across the Prairie and Arctic regions, the most common optimal version of the model was the +3 version, with a few stations having the +4 version as the optimal. The optimal version for the Forest and Mountain eco-climatic zones was much more variable. Since the degree of improvement was inconsistent even for stations in the same eco-climatic zones, the model's optimum threshold wind speed must be calculated for each specific station.

5.3 Influence of Direction

5.3.1 Methods

The focus was placed on severe blowing snow events for this analysis because of the importance of accurate forecasting of these events. Through use of the Climate Model, 8th revision created by Teresa Fisico (2003), severe blowing snow events, where the visibility was 3 SM or less, were broken down into 36 directional bins of 10 degrees each by the wind direction. This was done for each of the versions of the model where the constant in the threshold wind speed equation had been modified (-5 to +6). The results for each version of the model, for each of the 36 directional bins, were subtracted from the corresponding directional bin from the actual observations to give the critical value. When selecting the optimum model version for a given direction, the model version with the positive critical value closest to zero was chosen to guarantee that no blowing snow events were missed. For example, in Figure 5.5, for 50 degrees the +2 version of the model was the closest critical value, but it was not selected as the optimal version of the model for this direction because of its negative value, which meant that some blowing snow events were missed by that version of the model. For safety reasons, it was decided to select the version of the model which did not miss any of the severe events noted by the observers. In this case, the +1 version of the model was selected as the optimal version because it had the closest positive critical value to zero.

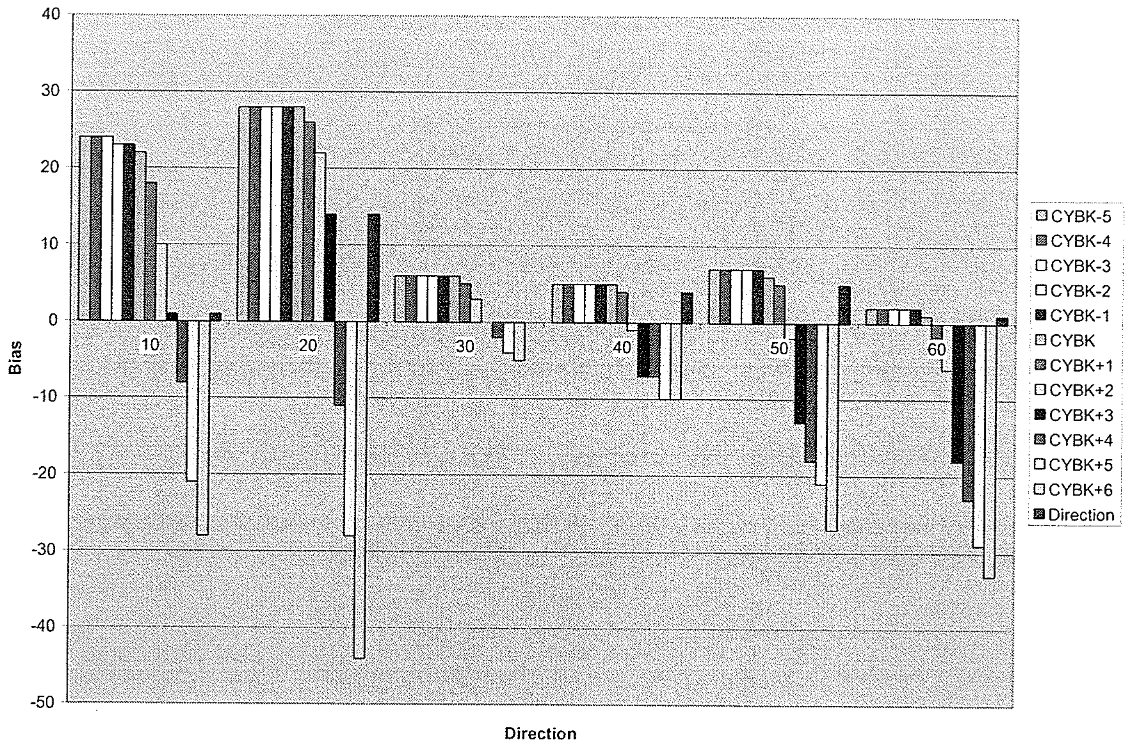

Figure 5.5 Critical values for the selection of the optimum threshold version of the model for Baker Lake for each directional bin.

Once the optimal versions of the model for each directional bin were selected, the model was modified to increase the threshold wind speed of the original version of the PIEKTUK model by a specific amount for each direction. The original data files were also modified to include wind direction so as to accommodate the new requirements of the model. The results on one Arctic station and one Prairie station were then analyzed.

5.3.2 Results

The analysis was completed for one Arctic station, Baker Lake, and one prairie station, Winnipeg. Initial analysis showed that adding in the influence of direction did improve the accuracy of the model, but not as much as adding 3 to the base calculation for the threshold wind speed. For Baker Lake, the CSI X2 value was originally about 45% but the +3 version of the model was 66.6% while the value for the dynamic version

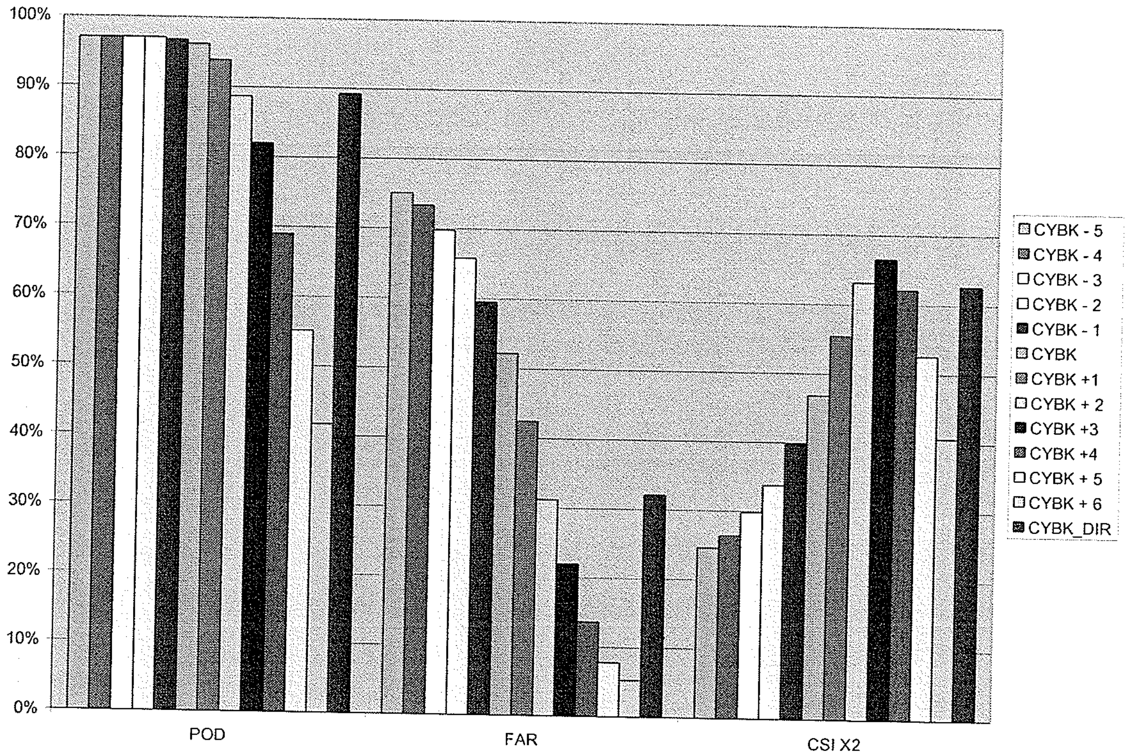

Figure 5.6 POD FAR and CSI X2 for Baker Lake for the analysis of the directional version of the model.

was 62.7% (Figure 5.6). A two-sample difference of proportions test was performed on the resulting CSI(X2) values and it was found that they were statistically different with a confidence of greater than 99.99%.

When only low visibility conditions were analyzed, the dynamic version of the model preformed worse than both the original version of the model, and also the +3 version which was the optimal version when all visibility categories were analyzed. The CSI for the +3 version was 72.4%, and the CSI value for the version including the influence of direction was 71.0%. Once again the two-sample difference of proportions test was performed on the resulting CSI(X2) values and it was found that they were statistically different with a confidence of 98.40%. The versions of the model with the greatest decrease in their threshold wind speed equations showed the highest CSI values. The results were almost identical for versions with a threshold wind speed +1 above the original model threshold wind speed to -5 below (Figure 5.7). The results for the -5 version of the model were also statistically different from the directional version with a confidence of greater than 99.99%.

When the results for Winnipeg were analyzed, some of the results differed from the Baker Lake analysis. For all visibility conditions, the +3 version of the model performed best, with a CSI value of 30.3%. The version including direction had a CSI value of 26.7%, and the original version of the model had a CSI value of 14.2% (Figure 5.8). The results were shown to be statistically different between the +3 and directional version of the model with 99.96% confidence. When just low visibility conditions were considered, the directional version of the model performed the best (CSI value of 43.8), with the +2 version of the model placing second (43.4%). The result for the directional version was shown to be statistically different from the +2 model version results with only 20.52% confidence. Once again, the lower threshold wind speed versions of the model had almost identical CSI values (Figure 5.9).

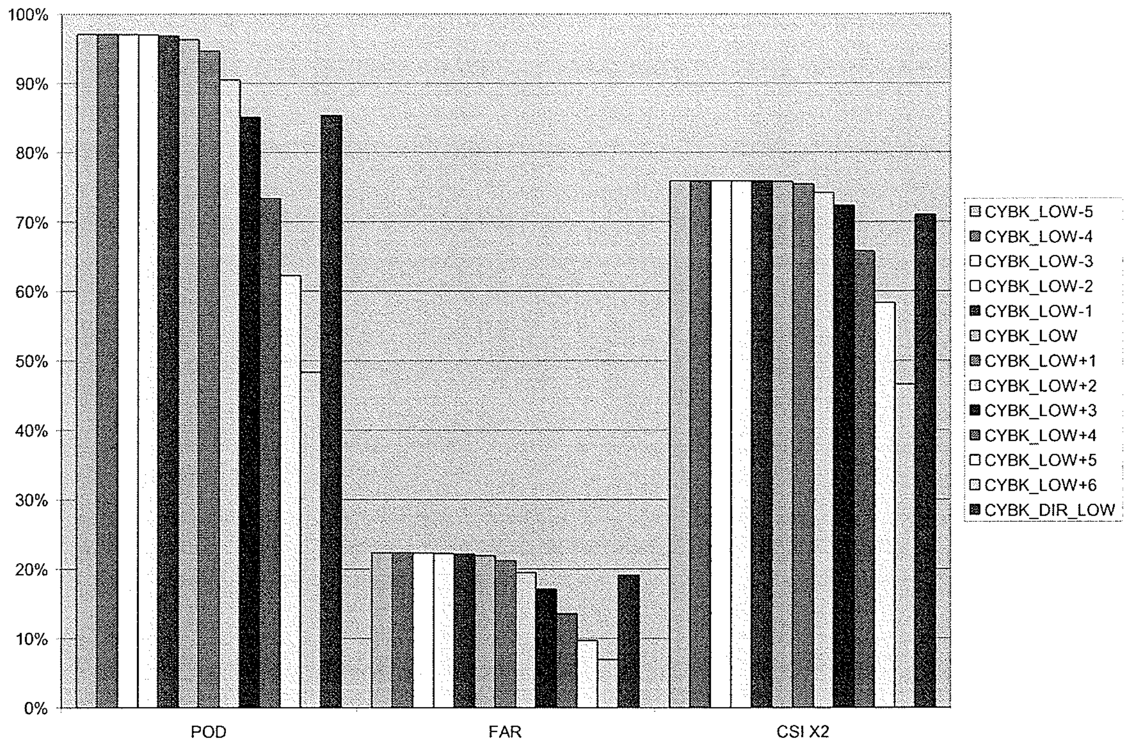

Figure 5.7 POD FAR and CSI X2 from the low visibility analysis of the direction dependant version of the model for Baker Lake.

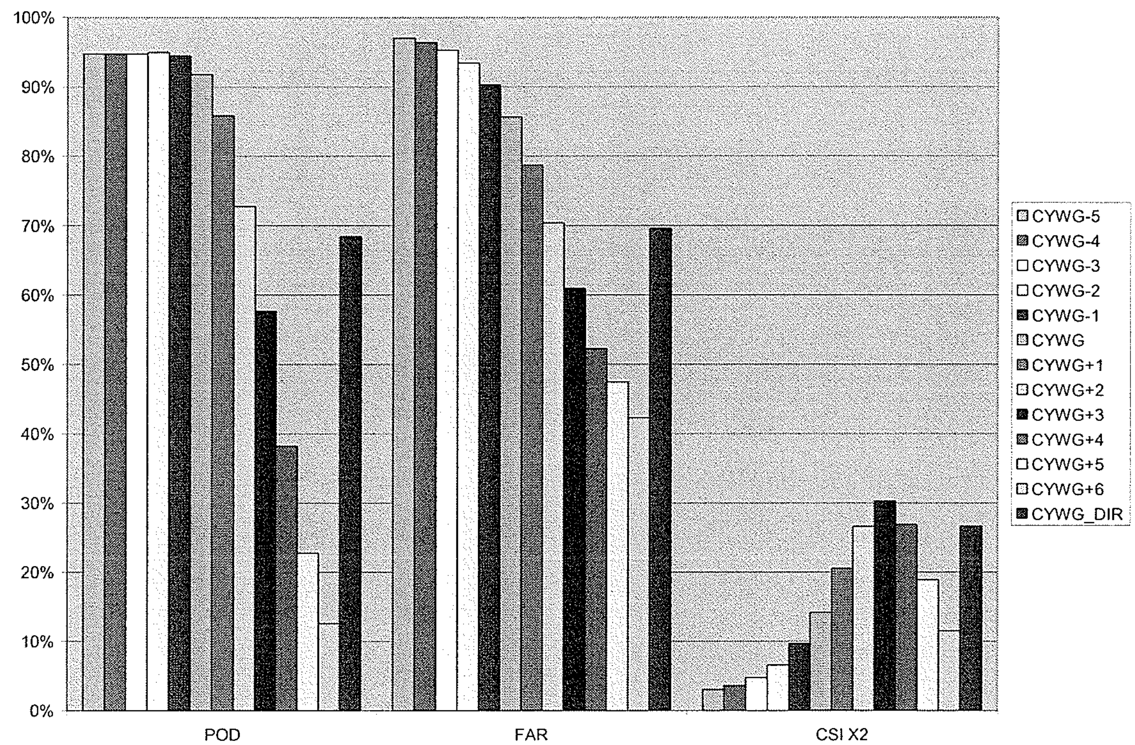

Figure 5.8 POD FAR and CSI X2 for the analysis of the directional version of the PIEKTUK model for Winnipeg

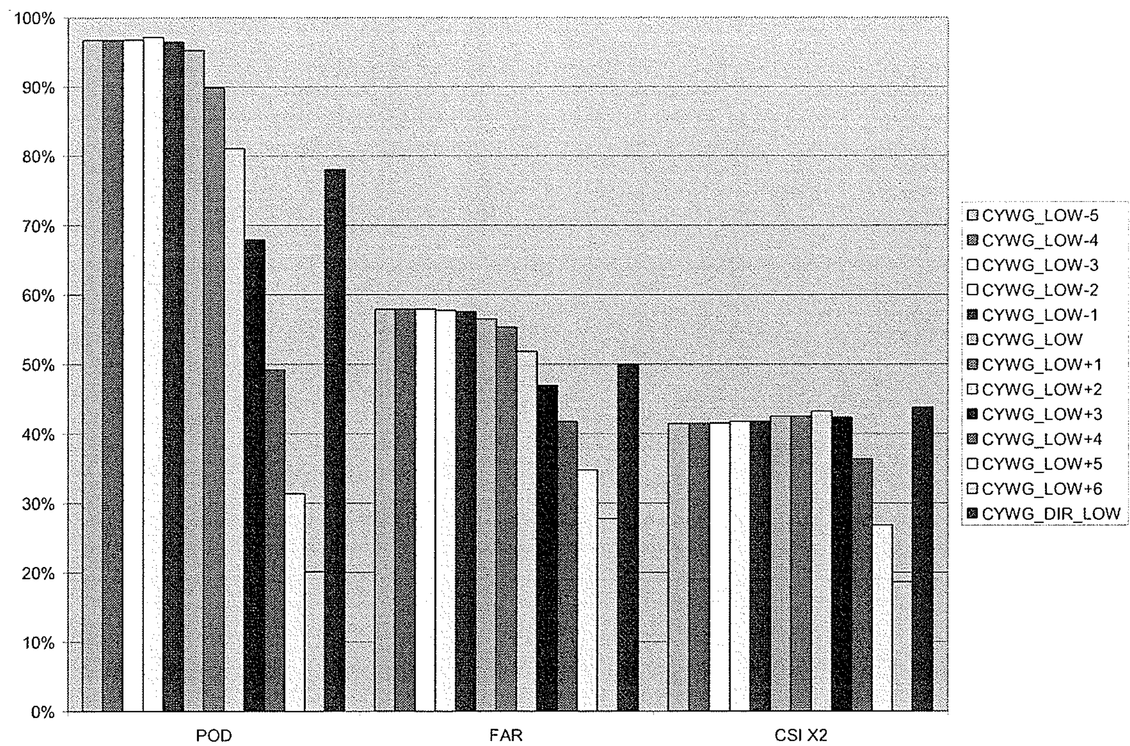

Figure 5.9 POD FAR and CSI X2 from the analysis of the direction dependant version of the model for Winnipeg for low visibility.

5.3.3 Conclusions

The dynamic version of the model does not seem to be an improvement over the version with the static optimal wind speed for all locations. With just severe visibility conditions included, there is a slight improvement shown by the Prairie station which has a low chance of being statistically significant, but no improvement was seen in the Arctic station. The lack of improvement in the dynamic version of the model might be due to the selection process for the optimum threshold wind speed for each direction. Instead of selecting the closest positive value when actual observations were subtracted from model predictions, using the closet value to 0 might provide better results. For example, in Figure 5.5 for the direction 40°, the model version with +1 added to the original threshold wind speed equation was selected because no blowing snow events were missed, while the version with +2 was closer to the actual observed results, but had missed a small number of events and was thereby eliminated as the optimal version to include in the directional dependent version of the model..

The Baker Lake analysis of low visibility indicated that more accurate forecasting of severe blowing snow events may be obtained if the constant in the threshold wind speed equation was decreased to one of the lower values selected for the analysis. While this may be beneficial to detect the severe events, the FAR over all blowing snow events using the same threshold wind speed versions of the model were close to 90%. For this station, it would be necessary to make a decision about which version would prove more useful in the prediction of blowing snow events, an increase in the CSI of approximately 5% for severe events, or a reduction in the FAR of around 50% for all blowing snow events.

6: PIEKTUK and the CASES Project

6.1 Introduction

In this chapter, I examined how well the PIEKTUK model predicted visibility conditions using data collected during the CASES project in 2004. The main question to be answered was whether or not the predictions of the model for visibility are close to the actual observed values.

6.2 Data and Methods

Data recorded during the Canadian Arctic Shelf Exchange Study (CASES) in 2003 and 2004 was also used to validate results obtained in the course of this thesis. The 10m wind speed was measured by a R.M Young model 05103 Wind Monitor. Visibility measurements were taken at 1m and 3m by Sentry visibility sensors. Wind measurements were taken every two seconds and the visibility measurements were taken every second. Measurements were averaged over five minutes, and stored in data loggers (CR23X and CR10X) (Huang et al., 2007). The visibility measurements were recorded from Day 28 to Day 84.

During this time period, there were five recorded events of blowing snow. The first commenced on Day 61 at 9:00, and lasted for 47 hours. The second began on Day 64 at 18:00, with a duration of 19 hours. The third event started on Day 66 at 20:00, and finished on day 67 at 7:00. The fourth lasted from Day 80, 21:00 to Day 81, 9:00. The final event recorded began on Day 82 at 22:00, and finished on Day 84 at 3:00. The CCGS Amundsen, which was the base station for the study was located at 70° 2.516' N, 126° 15.894W, and the site of the measurements was 1.5 km east of the ship (Deming et al, 2004). The site was located on a pan of uniform seasonal ice with a hard packed snow cover that ranged between 2 to 10 cm in thickness when the instruments were installed (Deming et al, 2004).

Since the PIEKTUK model defaults to visibility predictions at 2.5m, the observations from the CASES data sets were transformed to coincide with this value. This transformation was performed by another graduate student, Qiang Huang. The data was then graphed with data that had fixed temperatures of -20˚C, -30˚C, and -35˚C to compare the curves of the observed data to the curves of model output with set temperatures. The data was also graphed against different versions of the PIEKTUK model, which had been run on data that increased the observed wind speed from 5m s^{-1} to 19m s^{-1}, with a constant temperature of -20˚C. In these different model versions, the threshold wind speed was altered by increments of 1m s^{-1}, identical to the threshold wind speed testing that was used earlier in this project.

6.3 Results

Viewing the CASES data and the data sets with fixed temperature values, all data sets followed close to the same curve (Figure 6.1). The fixed temperature data sets have a sharper decrease in visibility with colder temperatures at the same wind speed. In comparison, the CASES data set has a sharper drop in visibility than any of the data sets with fixed temperatures but the coldest temperature follows the observed dataset most closely.

When the CASES data was compared to the versions of PIEKTUK with an incremental change in the "observed" wind speed, at lower wind speeds it was closest to the original version of the model. Once the observed wind speed reached 8m s^{-1}, the -1 version of the model most closely matched the observed data. Once past the 10m s^{-1} mark the CASES observations showed a greater decrease in visibility than any of the threshold versions of the model. The observations from CASES and the predictions from

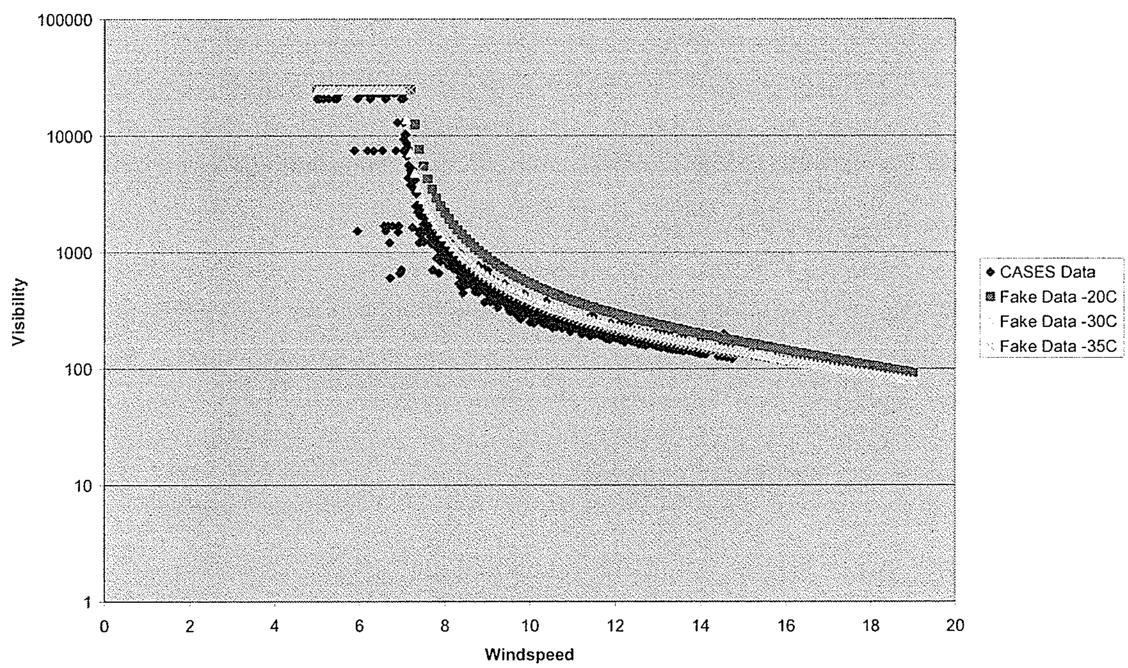

Figure 6.1 The CASES data set, compared to 3 temperature runs of the model with a constant increase in wind speed. Wind speed is measured in m s^{-1} and visibility is measured in m.

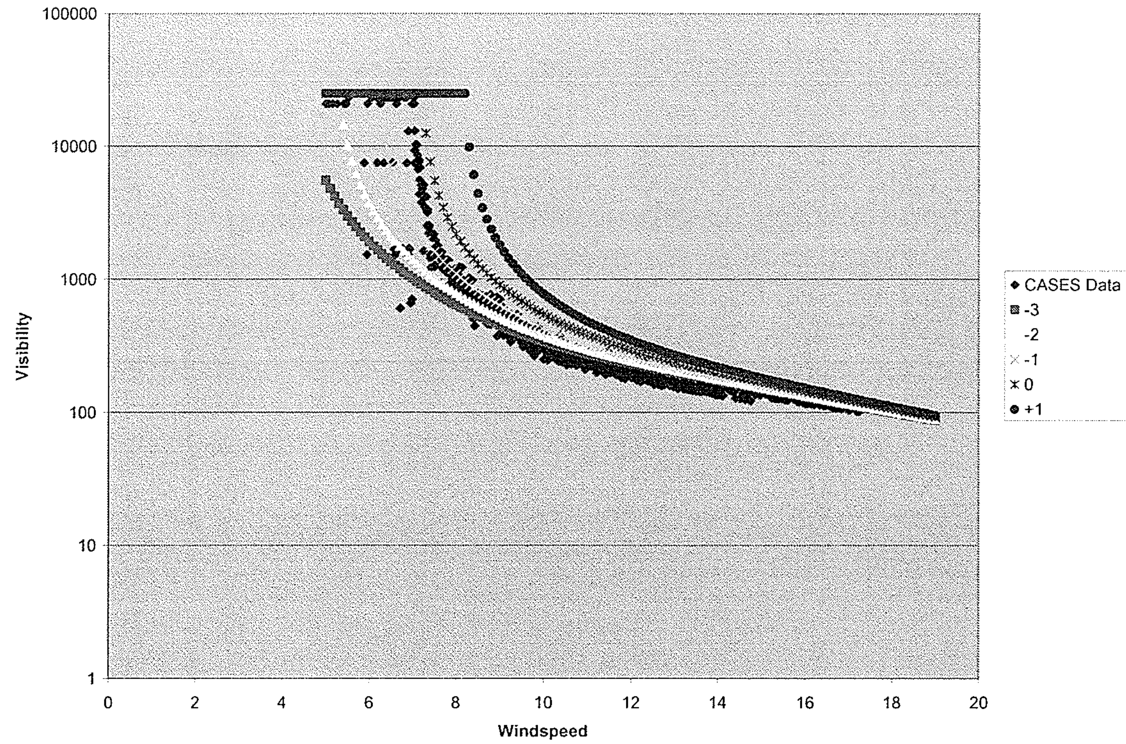

Figure 6.2 The CASES data set with threshold versions of the model with a constant temperature of -20°C. Wind speed is measured in m s^{-1} and visibility is measured in m.

Table 6.1 Chi-Square results comparing CASES observations to threshold versions of PIEKTUK

Model Version	Chi-square Value	Confidence that Model is Statistically Different
-3	809903.703	> 99.99%
-2	65914.777	> 99.99%
-1	884048.892	> 99.99%
Original	8256476.732	> 99.99%
+1	82058603.6	> 99.99%

the PIEKTUK models draw back together again at approximately 16m s^{-1} (Figure 6.2). To discover the best fit version of the model a chi-square goodness of fit test was performed (Table 6.1). While still statistically different from the data, the model version with the constant decreased by -2 fit the best, having the lowest chi-square value.

6.4 Conclusions

The curve defined by the PIEKTUK model does not accurately reflect the observed curve present in the data from the CASES project. Decreasing the temperature in the data created to show the specific curves of the model draws the curve of predictions closer to the observed data. Since temperatures observed in the CASES data ranged from -20˚C to a few events around -39˚C, with the majority occurring between -30˚C and -35˚C (average temperature of -31˚C), I concluded that the temperature equation present in the model needed to be adjusted to reflect the actual influence of temperature present in the CASES data.

When the observed data was compared to the threshold test of the model, the original version appeared the best able to predict the observed visibility close to the threshold wind speed. When the results were statistically analyzed it became apparent that while no version of the model could accurately represent the CASES data, the model version that had the threshold wind speed constant modified by -2 was the most accurate. Whether this change was due to having instruments record the visibility instead of observers, or just due to the fact that the measurements were taken out on the ice where surface roughness was minimal instead of on land where there is more surface variation remains unclear.

7: Conclusions and Future Research

7.1 Conclusions

From the evaluation of the PIEKTUK model over the Forest, Mountain, Prairie and Arctic regions, there is room for improvement in the predictive capabilities of the model. The current version of the model is not much use in forecasting for Mountain and Forest regions. For Prairie and Arctic regions it can be used as an indicator of whether blowing snow will occur or not, and for forecasting methods, it tends to err on the side of caution. The model rarely failed to predict a blowing snow event which was good from a public safety perspective. That said, too many incorrect predictions made which would lower the confidence of all predictions made by the model. There needs to be an effort made to reduce the number of false predictions of blowing snow made by the model. One way to do this would be to fine tune the model for each forecasting region with an optimal version for each location. For Prairie and Arctic eco-climatic zones a general version would be appropriate with all stations having an optimal version of the model when +3 or +4 are added to the constant in the threshold wind speed equation. For Forest and Mountain zones, a station specific model would be required due to the variations in the surrounding terrain, and other influences. When the visibility predictions made by PIEKTUK are examined, it becomes apparent that the model is unreliable for visibility forecasts in its current form.

Threshold wind speed testing has shown that to optimize the PIEKTUK model, the threshold wind speed should be raised by 3 for the Arctic and Prairie regions. Forest and Mountain regions are more dependent on their surrounding area, and to allow the model to perform to the best of its ability each station needs to be evaluated separately.

Breaking down blowing snow events into 10° directional bins revealed that the model performance varies by direction. After creating and testing a dynamic version of the model where the threshold wind speed was determined by direction, the results did not show an improvement in the predictive capabilities of the model than the adjustment of the constant in the threshold wind speed equation. For both stations, Winnipeg and Baker Lake, when all visibility categories were considered, the +3 version of the model preformed better that the directional version. Part of this could be the way the optimal wind speed was selected for each direction. The threshold wind speed that had the lowest positive value after the actual observations were subtracted was selected as the optimal version of the model. This emphasis on not missing any severe blowing snow events excluded versions of the model where the value after subtraction of the actual events was closer to the number of observed events than the version selected as optimal, but the resulting value was negative, indicating that version of the model missed some of the severe events. The rational behind the selection of the optimal version was to avoid underprediction because of safety concerns for forecasting, but this may have served to decrease the overall predictive capability of the directional dependant model.

The CSI(X2) results for the low visibility analysis of the directional dependant version of the model, and the incremental threshold wind speed versions showed a curious flatness in the graphs for Baker Lake which had lower threshold wind speed values than the original model. One possible reason for this result is the data for the predictions in question are faulty in recording or observation. Due to the nature of the definition of blowing snow, unless the visibility observations are made by an instrument, it is a judgment call by the observer, and this allows the possibility of human error. This error could affect all of the results from this thesis, the effect only being visible when the low visibility analysis was performed. Other than the visibility observations, errors in the wind speed measurements or temperature recording could influence the result of the model. These could be manual errors in recording the data, transferring it from one storage method to another (written records to digital), or errors in the instruments that produced the measurements. The lowest threshold wind speed tested for the model had a constant of 4.43 (5.1). Most blowing snow events should be caught by that version of the model. It is likely that any events that were missed by this version of the model were either recorded incorrectly by the observer, or entered incorrectly in the data set.

When the predictions made by PIEKTUK on the CASES data set were compared to the actual measured visibility values, a discrepancy in the visibility curve graphed by the model was revealed. The shift in the default prediction curve, when influenced only by temperature changes, did not accurately mimic the actual observations. Temperatures in the CASES data were almost always within the temperature zones graphed, but the CASES data seemed to be observed at a colder temperature, if extrapolation of the curve progression is correct. My research has identified areas where further research is needed. My attempts improved the results from the PIEKTUK model slightly, but there is still more room for improvement.

7.2 Future Research

Continuing on the path of my thesis, a second version of the direction dependent version of the model may provide more accurate results. Instead of using the version of the model from the threshold wind speed testing that had the smallest positive value after the actual observations were subtracted from the model predictions, using the closet value to 0 may improve the predictive capability of the model more. Repeating both the analysis completed for Winnipeg and Baker Lake for other stations could also provide valuable information on the benefit of including the influence of direction into the model. This would give further insight into the apparent "flatness" in the graphs for low visibility during the threshold testing of the model. The reason for the levelling off of the probability of detection for the lower threshold wind speed versions as compared to the higher threshold wind speed versions is not apparent. Discovering the reason for this result could provide another way to improve the model.

From the analysis of the CASES data and the model, it is apparent that the curve defined by the model did not correctly represent the decrease in visibility compared to wind speed. Analysis of other variables may indicate that they are statistically significant in the prediction of visibility in blowing snow.

More testing, like the threshold testing and simple graphing of data, of the model on instrument recorded data would also be beneficial in determining how detrimental human error is to the performance of the model. This would remove any human error or bias in the observations of visibility, and possibly give some insight into the extent of errors in existing data sets.

Appendix A

Initial analysis by station with null weather events (X) and without (X2)

Prairie	POD	FAR	CSI(X)
CYWG	99.87%	7.72%	92.72%
CYPG	99.91%	5.98%	93.93%
CYBR	99.93%	5.40%	94.54%
CYEN	99.91%	6.86%	93.14%
CYMJ	99.93%	5.37%	94.54%
CYQV	99.90%	5.37%	95.99%
CYQW	99.91%	3.93%	95.99%
CYXE	99.97%	3.83%	96.14%
CYYN	99.95%	12.36%	87.61%
CYQR	99.89%	8.48%	91.43%

Prairie	POD	FAR	CSI(X2)
CYWG	91.78%	85.62%	0.14%
CYPG	93.29%	82.94%	16.85%
CYBR	92.46%	86.90%	12.96%
CYEN	90.69%	89.35%	10.53%
CYMJ	96.16%	84.06%	15.84%
CYQV	89.41%	86.69%	13.10%
CYQW	88.04%	85.42%	14.29%
CYXE	93.21%	93.20%	9.73%
CYYN	96.38%	92.04%	7.93%
CYQR	92.40%	86.91%	12.95%

Arctic

CYCO	98.94%	16.50%	82.76%
CYBK	99.19%	18.10%	81.35%
CYRB	79.02%	20.98%	65.32%
CYYQ	99.54%	14.01%	85.65%
CYCB	98.99%	18.00%	81.32%
CYFB	98.89%	14.61%	84.58%
CYIO	98.81%	39.62%	59.94%
CYTE	99.20%	15.28%	84.14%
CYUX	99.15%	19.29%	80.15%
CYZS	99.48%	15.77%	83.86%

Arctic

CYCO	84.83%	76.66%	22.40%
CYBK	96.11%	52.22%	46.87%
CYRB	48.37%	51.63%	31.90%
CYYQ	94.71%	66.13%	33.24%
CYCB	94.31%	56.60%	42.30%
CYFB	89.50%	64.18%	34.38%
CYIO	33.39%	99.09%	0.89%
CYTE	87.50%	76.11%	23.10%
CYUX	94.94%	59.92%	39.24%
CYZS	95.89%	60.44%	38.90%

Forest

CYDN	100.00%	10.03%	90.00%
CYPE	100.00%	0.62%	99.38%
CYHY	99.96%	2.49%	97.48%
CYFS	99.94%	0.74%	99.21%
CYSM	99.86%	1.53%	98.33%
CYVC	99.95%	0.89%	99.06%
CYXY	99.99%	6.53%	93.46%
CYZF	99.96%	4.23%	95.74%
CYVQ	99.76%	4.87%	94.91%
CYPA	99.97%	2.86%	97.11%
CYEV	99.84%	0.53%	99.32%

Forest

CYDN	99.56%	91.84%	8.16%
CYPE	93.02%	94.05%	5.93%
CYHY	80.97%	94.22%	5.71%
CYFS	65.88%	87.37%	11.85%
CYSM	62.53%	86.56%	12.44%
CYVC	57.00%	93.72%	5.99%
CYXY	86.76%	99.02%	0.98%
CYZF	83.67%	95.50%	4.47%
CYVQ	88.17%	74.46%	24.69%
CYPA	75.17%	97.20%	2.77%
CYEV	60.96%	68.18%	26.43%

Mountain

CYQF	99.99%	1.66%	98.33%
CYYC	99.99%	1.82%	98.17%
CYXH	99.99%	1.40%	98.59%
CYEG	99.99%	1.94%	98.05%

Mountain

CYQF	89.57%	95.49%	4.48%
CYYC	88.69%	96.00%	3.97%
CYXH	82.86%	95.84%	4.16%
CYEG	94.70%	95.17%	4.81%

Appendix B

Wind speed threshold results by station by eco-climatic zone

Prairie eco-climatic zone

Station CYPG	Visibility Threshold	POD	FAR	CSI X
	9.6	0.93514	0.837756	0.160438
	8	0.93757	0.851989	0.146567
	6.4	0.941176	0.868757	0.130175
	4.8	0.944984	0.886624	0.112633
	3.2	0.961798	0.903885	0.095749
	1.6	0.977477	0.928899	0.070985
	0.8	0.923077	0.954745	0.045085
	0.4	0.894737	0.968105	0.031776
	0	0	0	0
	1	0.913669	0.939667	0.059991

Station CYQR	Visibility Threshold	POD	FAR	CSI X
	9.6	0.864597	0.874207	0.123363
	8	0.865315	0.88244	0.115448
	6.4	0.855833	0.453723	0.500244
	4.8	0.837784	0.909315	0.08912
	3.2	0.817844	0.922271	0.076407
	1.6	0.753704	0.935108	0.063544
	0.8	0.708738	0.937978	0.060481
	0.4	0.680412	0.944068	0.0545
	0	0	0	0
	1	0.72104	0.930964	0.06724

Station CYWG	Visibility Threshold	POD	FAR	CSI X
	9.6	0.899183	0.870993	0.127168
	8	0.898949	0.888163	0.110449
	6.4	0.905812	0.906321	0.092775
	4.8	0.907507	0.926285	0.073165
	3.2	0.890772	0.942998	0.056606
	1.6	0.821293	0.965329	0.034411
	0.8	0.75	0.983562	0.016349
	0.4	0.882353	0.988198	0.011783
	0	0	0	0
	1	0.755102	0.975361	0.024444

Station	Visibility			
CYEN	Threshold	POD	FAR	CSI X
	9.6	0.821622	0.894493	0.103144
	8	0.81459	0.904422	0.093543
	6.4	0.805461	0.913214	0.085004
	4.8	0.79156	0.919673	0.078663
	3.2	0.742373	0.936356	0.062269
	1.6	0.665746	0.951839	0.047024
	0.8	0.476684	0.966214	0.032578
	0.4	0.291667	0.975	0.023569
	0	0	0	0
	1	0.568841	0.954281	0.044188

Station	Visibility			
CYMJ	Threshold	POD	FAR	CSI X
	9.6	0.955962	0.847029	0.1519
	8	0.959169	0.856444	0.142684
	6.4	0.967715	0.870096	0.129344
	4.8	0.972364	0.885515	0.114114
	3.2	0.973788	0.901276	0.098463
	1.6	0.960954	0.920865	0.078882
	0.8	0.962343	0.925081	0.0747
	0.4	0.899083	0.904016	0.094961
	0	0	0	0
	1	0.957746	0.912258	0.087404

Station	Visibility			
CYQV	Threshold	POD	FAR	CSI X
	9.6	0.776355	0.857787	0.136616
	8	0.77323	0.870986	0.124311
	6.4	0.776786	0.883623	0.112611
	4.8	0.764331	0.901619	0.095484
	3.2	0.732943	0.912047	0.085222
	1.6	0.649852	0.922697	0.074212
	0.8	0.494382	0.932773	0.062902
	0.4	0.239437	0.947692	0.044855
	0	0	0	0
	1	0.544402	0.917108	0.077515

Station	Visibility			
CYXE	Threshold	POD	FAR	CSI X
	9.6	0.835141	0.913191	0.085347
	8	0.81407	0.924791	0.073939
	6.4	0.789474	0.938032	0.060961
	4.8	0.771084	0.949099	0.050144
	3.2	0.689655	0.962535	0.036844
	1.6	0.454545	0.980218	0.019324
	0.8	0.27451	0.984683	0.014721
	0.4	0.3	0.953608	0.04186
	0	0	0	0
	1	0.318841	0.982085	0.017255

Station	Visibility			
CYYN	Threshold	POD	FAR	CSI X
	9.6	0.715992	0.875823	0.118347
	8	0.716704	0.887214	0.107972
	6.4	0.711277	0.88963	0.105637
	4.8	0.706053	0.914798	0.082284
	3.2	0.685808	0.927262	0.070392
	1.6	0.617202	0.941809	0.056164
	0.8	0.483993	0.951621	0.046006
	0.4	0.340478	0.945138	0.049592
	0	0	0	0
	1	0.557538	0.94016	0.057127

Station	Visibility			
CYQW	Threshold	POD	FAR	CSI X
	9.6	0.776355	0.857787	0.136616
	8	0.77323	0.870986	0.124311
	6.4	0.776786	0.883623	0.112611
	4.8	0.764331	0.901619	0.095484
	3.2	0.732943	0.912047	0.085222
	1.6	0.649852	0.922697	0.074212
	0.8	0.494382	0.932773	0.062902
	0.4	0.239437	0.947692	0.044855
	0	0	0	0
	1	0.544402	0.917108	0.077515

Forest eco-climatic zone

Station	Visibility			
CYDN	Threshold	POD	FAR	CSI X
	9.6	0.96124	0.926242	0.07354
	8	0.957478	0.933537	0.066268
	6.4	0.951786	0.944375	0.055469
	4.8	0.932961	0.963465	0.036439
	3.2	0.898305	0.974696	0.025232
	1.6	0.833333	0.980886	0.019042
	0.8	0.519231	0.992738	0.007213
	0.4	0.272727	0.993594	0.006298
	0	0	0	0
	1	0.768519	0.981941	0.017961

Station	Visibility			
CYFS	Threshold	POD	FAR	CSI X
	9.6	0.360656	0.886158	0.094726
	8	0.34359	0.904422	0.08082
	6.4	0.325153	0.917188	0.070667
	4.8	0.297521	0.9401	0.052478
	3.2	0.25	0.961315	0.034662
	1.6	0.066667	0.986441	0.011396
	0.8	0	1	0
	0.4	0	1	0
	0	0	0	0
	1	0.017857	0.994536	0.004202

Station	Visibility			
CYHY	Threshold	POD	FAR	CSI X
	9.6	0.69378	0.946554	0.052215
	8	0.67052	0.953488	0.045472
	6.4	0.651613	0.957687	0.041376
	4.8	0.650407	0.964586	0.034752
	3.2	0.58427	0.973361	0.026144
	1.6	0.461538	0.979275	0.020236
	0.8	0.454545	0.979508	0.02
	0.4	0.333333	0.976378	0.022556
	0	0	0	0
	1	0.439024	0.974504	0.024691

Station	Visibility			
CYPE	Threshold	POD	FAR	CSI X
	9.6	0.596491	0.935361	0.061931
	8	0.58	0.941176	0.05642
	6.4	0.564103	0.95186	0.046414
	4.8	0.558824	0.951407	0.046798
	3.2	0.5	0.946619	0.050676
	1.6	0.318182	0.95	0.045161
	0.8	0.0625	0.975	0.018182
	0.4	0	1	0
	0	0	0	0
	1	0.157895	0.957143	0.034884

Station	Visibility			
CYSM	Threshold	POD	FAR	CSI X
	9.6	0.077529	0.879215	0.04956
	8	0.071361	0.9	0.043453
	6.4	0.067806	0.909221	0.040382
	4.8	0.062684	0.933229	0.033412
	3.2	0.032741	0.965619	0.017057
	1.6	0.010539	0.983577	0.006461
	0.8	0	1	0
	0.4	0	1	0
	0	0	0	0
	1	0.00123	0.996885	0.000883

Station	Visibility			
CYVC	Threshold	POD	FAR	CSI X
	9.6	0.414141	0.942577	0.053109
	8	0.373494	0.954412	0.04235
	6.4	0.342466	0.961059	0.036232
	4.8	0.26087	0.979239	0.019608
	3.2	0.181818	0.986928	0.012346
	1.6	0	1	0
	0.8	0	1	0
	0.4	0	1	0
	0	0	0	0
	1	0	1	0

Station CYVQ	Visibility Threshold	POD	FAR	CSI X
	9.6	0.86875	0.776572	0.216132
	8	0.777422	0.809009	0.181089
	6.4	0.779135	0.833132	0.159331
	4.8	0.7366	0.899541	0.096976
	3.2	0.668763	0.926311	0.071094
	1.6	0.450382	0.964829	0.033724
	0.8	0.183206	0.989021	0.010467
	0.4	0.057471	0.995112	0.004525
	0	0	0	0
	1	0.387931	0.966292	0.032006

Station CYZF	Visibility Threshold	POD	FAR	CSI X
	9.6	0.457831	0.675214	0.234568
	8	0.457143	0.679417	0.23219
	6.4	0.463415	0.712665	0.215603
	4.8	0.477912	0.761523	0.189189
	3.2	0.441341	0.808252	0.154297
	1.6	0.307018	0.863813	0.104167
	0.8	0.066667	0.973451	0.019355
	0.4	0	1	0
	0	0	0	0
	1	0.134146	0.929936	0.048246

Station CYEV	Visibility Threshold	POD	FAR	CSI X
	9.6	0.457831	0.675214	0.234568
	8	0.457143	0.679417	0.23219
	6.4	0.463415	0.712665	0.215603
	4.8	0.477912	0.761523	0.189189
	3.2	0.441341	0.808252	0.154297
	1.6	0.307018	0.863813	0.104167
	0.8	0.066667	0.973451	0.019355
	0.4	0	1	0
	0	0	0	0
	1	0.134146	0.929936	0.048246

Station	Visibility			
CYPA	Threshold	POD	FAR	CSI X
	9.6	0.397849	0.976788	0.022424
	8	0.357616	0.982405	0.017056
	6.4	0.258621	0.990037	0.009687
	4.8	0.224299	0.991167	0.008571
	3.2	0.170213	0.993031	0.00674
	1.6	0.084337	0.994807	0.004916
	0.8	0.030769	0.996303	0.003311
	0.4	0	1	0
	0	0	0	0
	1	0.084337	0.990463	0.008642

Station	Visibility			
CYEG	Threshold	POD	FAR	CSI X
	9.6	0.753731	0.954931	0.044415
	8	0.728814	0.96035	0.039073
	6.4	0.686869	0.967118	0.032396
	4.8	0.623377	0.974277	0.02533
	3.2	0.52459	0.979811	0.019827
	1.6	0.27027	0.98954	0.010173
	0.8	0.090909	0.994911	0.004843
	0.4	0	1	0
	0	0	0	0
	1	0.181818	0.989189	0.010309

Arctic eco-climatic zone

Station	Visibility			
CYCO	Threshold	POD	FAR	CSI X
	9.6	0.832638	0.789103	0.202321
	8	0.836172	0.796711	0.195502
	6.4	0.840596	0.809783	0.183594
	4.8	0.854839	0.832588	0.162785
	3.2	0.869058	0.858865	0.138196
	1.6	0.857295	0.862275	0.134638
	0.8	0.847788	0.871994	0.125131
	0.4	0.832776	0.859797	0.136364
	0	0	0	0
	1	0.84371	0.850854	0.145137

Station	Visibility			
CYBK	Threshold	POD	FAR	CSI X
	9.6	0.958569	0.536163	0.454721
	8	0.959177	0.547109	0.444327
	6.4	0.960225	0.565802	0.426527
	4.8	0.961332	0.59903	0.394606
	3.2	0.961939	0.624458	0.370043
	1.6	0.958095	0.645486	0.349101
	0.8	0.960772	0.682553	0.313385
	0.4	0.946959	0.700289	0.294762
	0	0	0	0
	1	0.957997	0.642268	0.352207

Station	Visibility			
CYRB	Threshold	POD	FAR	CSI X
	9.6	0.952389	0.537132	0.4524
	8	0.952233	0.564488	0.426201
	6.4	0.95188	0.597764	0.39422
	4.8	0.951334	0.657329	0.336767
	3.2	0.953375	0.70904	0.286878
	1.6	0.952601	0.779375	0.218229
	0.8	0.682558	0.86359	0.128273
	0.4	0.957413	0.906088	0.093521
	0	0	0	0
	1	0.952951	0.808565	0.189642

Station	Visibility			
CYYQ	Threshold	POD	FAR	CSI X
	9.6	0.938878	0.66282	0.329938
	8	0.909836	0.778884	0.216374
	6.4	0.933247	0.749914	0.245691
	4.8	0.952726	0.710732	0.285174
	3.2	0.95256	0.734849	0.261695
	1.6	0.967351	0.787674	0.210815
	0.8	0.972305	0.861393	0.138062
	0.4	0.982143	0.883227	0.116525
	0	0	0	0
	1	0.966602	0.815292	0.183537

Station	Visibility			
CYCB	Threshold	POD	FAR	CSI X
	9.6	0.851761	0.552559	0.415115
	8	0.858221	0.562665	0.407867
	6.4	0.865829	0.573769	0.399823
	4.8	0.875687	0.609848	0.369677
	3.2	0.888993	0.641039	0.343562
	1.6	0.899878	0.685486	0.303881
	0.8	0.897738	0.743219	0.249483
	0.4	0.891675	0.760668	0.23257
	0	0	0	0
	1	0.901027	0.710094	0.280959

Station	Visibility			
CYFB	Threshold	POD	FAR	CSI X
	9.6	0.890864	0.661522	0.325001
	8	0.889579	0.677492	0.310094
	6.4	0.896873	0.706701	0.28373
	4.8	0.903194	0.743174	0.249946
	3.2	0.899755	0.784059	0.210868
	1.6	0.896075	0.835642	0.161284
	0.8	0.869403	0.890374	0.10785
	0.4	0.813859	0.905311	0.092681
	0	0	0	0
	1	0.884555	0.859514	0.137956

Station	Visibility			
CYIO	Threshold	POD	FAR	CSI X
	9.6	0.335338	0.957627	0.03909
	8	0.331835	0.962822	0.034589
	6.4	0.332248	0.966944	0.030996
	4.8	0.333528	0.973229	0.025412
	3.2	0.324924	0.979325	0.019824
	1.6	0.309051	0.984684	0.014809
	0.8	0.22314	0.990819	0.008897
	0.4	0.14554	0.993577	0.006189
	0	0	0	0
	1	0.249326	0.988534	0.011084

Station	Visibility			
CYTE	Threshold	POD	FAR	CSI X
	9.6	0.343047	0.667187	0.203263
	8	0.343863	0.690935	0.194413
	6.4	0.347174	0.713164	0.186334
	4.8	0.34471	0.764619	0.162617
	3.2	0.336024	0.822725	0.131286
	1.6	0.331933	0.89046	0.089752
	0.8	0.285714	0.941916	0.050719
	0.4	0.205534	0.952468	0.040154
	0	0	0	0
	1	0.328829	0.921251	0.067844

Station	Visibility			
CYUX	Threshold	POD	FAR	CSI X
	9.6	0.845766	0.569767	0.398934
	8	0.852358	0.581281	0.390404
	6.4	0.8572	0.593578	0.38065
	4.8	0.871036	0.624486	0.355736
	3.2	0.884401	0.646222	0.338142
	1.6	0.892068	0.698878	0.290537
	0.8	0.889319	0.749649	0.242786
	0.4	0.877653	0.81407	0.181232
	0	0	0	0
	1	0.893994	0.711994	0.278495

Mountain eco-climatic zone

Station CYQF	Visibility Threshold	POD	FAR	CSI X
	9.6	0.396552	0.954115	0.04289
	8	0.361502	0.960207	0.03718
	6.4	0.326633	0.964227	0.033316
	4.8	0.293478	0.967391	0.030235
	3.2	0.183544	0.978848	0.019333
	1.6	0.119718	0.980324	0.017189
	0.8	0.076923	0.983645	0.013672
	0.4	0.048387	0.973913	0.017241
	0	0	0	0
	1	0.119718	0.969479	0.024927

Station CYXH	Visibility Threshold	POD	FAR	CSI X
	9.6	0.544118	0.95898	0.039657
	8	0.53211	0.966474	0.032566
	6.4	0.53012	0.972823	0.026538
	4.8	0.460317	0.979959	0.019581
	3.2	0.385965	0.981403	0.018062
	1.6	0.205128	0.988372	0.011127
	0.8	0	1	0
	0.4	0	1	0
	0	0	0	0
	1	0.090909	0.990964	0.008287

Station CYYC	Visibility Threshold	POD	FAR	CSI X
	9.6	0.633094	0.961182	0.037964
	8	0.618321	0.96298	0.036193
	6.4	0.605505	0.96833	0.03103
	4.8	0.543478	0.973945	0.025497
	3.2	0.444444	0.9801	0.019417
	1.6	0.22	0.989484	0.010138
	0.8	0.151515	0.990079	0.009398
	0.4	0.428571	0.97931	0.020134
	0	0	0	0
	1	0.204082	0.984802	0.014347

Station	Visibility			
CYEG	Threshold	POD	FAR	CSI X
	9.6	0.753731	0.954931	0.044415
	8	0.728814	0.96035	0.039073
	6.4	0.686869	0.967118	0.032396
	4.8	0.623377	0.974277	0.02533
	3.2	0.52459	0.979811	0.019827
	1.6	0.27027	0.98954	0.010173
	0.8	0.090909	0.994911	0.004843
	0.4	0	1	0
	0	0	0	0
	1	0.181818	0.989189	0.010309

Appendix C

Visibility ranges by station by eco-climatic zone

Prairie eco-climatic zone

Station	Visibility			
CYPG	Range	POD	FAR	CSI X
	9.6	0.307692	0.982063	0.017241
	8	0.1	0.995708	0.004132
	6.4	0	1	0
	4.8	0.666667	0.987152	0.012766
	3.2	1	0.990055	0.009945
	1.6	0.7	0.981115	0.018733
	0.8	0.909091	0.990128	0.009862
	0.4	0.973684	0.965993	0.033976
	0.2	0	0	0

Station	Visibility			
CYQR	Range	POD	FAR	CSI X
	9.6	0	1	0
	8	0	1	0
	6.4	0	1	0
	4.8	0	1	0
	3.2	0.714286	0.996085	0.003909
	1.6	0.8	0.995754	0.004242
	0.8	0.8	0.995974	0.004022
	0.4	0.987342	0.967715	0.032271
	0.2	0	0	0

Station	Visibility			
CYWG	Range	POD	FAR	CSI X
	9.6	0.166667	0.996454	0.003484
	8	0.8	0.985455	0.014493
	6.4	0	1	0
	4.8	0.4	0.996979	0.003008
	3.2	0.777778	0.99421	0.00578
	1.6	0.928571	0.992969	0.007027
	0.8	0.8	0.997875	0.002124
	0.4	0.761905	0.993881	0.006107
	0.2	0	0	0

Station CYBR	Visibility Range	POD	FAR	CSI X
	9.6	0.2	0.996241	0.003704
	8	0	1	0
	6.4	0	1	0
	4.8	0.4	0.992687	0.007233
	3.2	0.5	0.995229	0.004748
	1.6	1	0.993192	0.006808
	0.8	0.833333	0.995479	0.004517
	0.4	0.916667	0.969359	0.030556
	0.2	0	0	0

Station CYEN	Visibility Range	POD	FAR	CSI X
	9.6	0	1	0
	8	0	1	0
	6.4	0	1	0
	4.8	0	1	0
	3.2	0.818182	0.99258	0.007407
	1.6	0.428571	0.998087	0.001908
	0.8	0.833333	0.993723	0.00627
	0.4	0.981481	0.971164	0.02882
	0.2	0	0	0

Station CYMJ	Visibility Range	POD	FAR	CSI X
	9.6	0.1	0.994898	0.004878
	8	0	1	0
	6.4	0.5	0.996875	0.003115
	4.8	0.375	0.995161	0.0048
	3.2	0.529412	0.992084	0.00786
	1.6	0.625	0.991329	0.008626
	0.8	0.315789	0.99654	0.003434
	0.4	0.873016	0.947394	0.052207
	0.2	0	0	0

Station	Visibility			
CYQV	Range	POD	FAR	CSI X
	9.6	0.166667	0.995349	0.004545
	8	0	1	0
	6.4	0.428571	0.991573	0.008333
	4.8	0.285714	0.997106	0.002874
	3.2	0.625	0.995693	0.004296
	1.6	0.7	0.994693	0.005295
	0.8	0.666667	0.992278	0.007692
	0.4	0.9375	0.970732	0.029211
	0.2	0	0	0

Station	Visibility			
CYXE	Range	POD	FAR	CSI X
	9.6	0	1	0
	8	0.333333	0.993631	0.006289
	6.4	0	1	0
	4.8	0.5	0.997753	0.002242
	3.2	0.5	0.993207	0.006748
	1.6	1	0.993182	0.006818
	0.8	1	0.997046	0.002954
	0.4	0.333333	0.994465	0.005474
	0.2	0	0	0

Station	Visibility			
CYYN	Range	POD	FAR	CSI X
	9.6	0	1	0
	8	0.166667	0.997396	0.002571
	6.4	0.111111	0.998299	0.001678
	4.8	0.272727	0.997076	0.002901
	3.2	0.68	0.9913	0.008665
	1.6	0.761905	0.993636	0.006352
	0.8	0.592593	0.992431	0.007529
	0.4	0.92381	0.956561	0.043284
	0.2	0	0	0

Station	Visibility			
CYQW	Range	POD	FAR	CSI X
	9.6	0	1	0
	8	0	1	0
	6.4	0	1	0
	4.8	0.333333	0.993534	0.006383
	3.2	0.307692	0.995311	0.00464
	1.6	0.65	0.988992	0.010943
	0.8	0.75	0.98229	0.017606
	0.4	1	0.917453	0.082547
	0.2	0	0	0

Forest eco-climatic zone

Station CYDN	Visibility Range	POD	FAR	CSI X
	9.6	0	1	0
	8	0	1	0
	6.4	0	1	0
	4.8	0	1	0
	3.2	0	1	0
	1.6	0	1	0
	0.8	0.5	0.999476	0.000524
	0.4	0.875	0.997395	0.002604
	0.2	0	0	0

Station CYFS	Visibility Range	POD	FAR	CSI X
	9.6	0	1	0
	8	0.2	0.987013	0.012346
	6.4	0	1	0
	4.8	0	1	0
	3.2	0.333333	0.993377	0.006536
	1.6	1	0.951456	0.048544
	0.8	0	1	0
	0.4	0	1	0
	0.2	0	0	0

Station CYHY	Visibility Range	POD	FAR	CSI X
	9.6	0.222222	0.990148	0.009524
	8	0	1	0
	6.4	0	1	0
	4.8	1	0.995283	0.004717
	3.2	0.375	0.994718	0.005236
	1.6	1	0.992661	0.007339
	0.8	0.8	0.989501	0.010471
	0.4	1	0.986842	0.013158
	0.2	0	0	0

Station CYPE	Visibility Range	POD	FAR	CSI X
	9.6	0	1	0
	8	1	0.96875	0.03125
	6.4	0	1	0
	4.8	0	1	0
	3.2	0	1	0
	1.6	0	1	0
	0.8	1	0.943396	0.056604
	0.4	0	1	0
	0.2	0	0	0

Station CYSM	Visibility Range	POD	FAR	CSI X
	9.6	0.333333	0.988889	0.01087
	8	0.2	0.985507	0.013699
	6.4	0	1	0
	4.8	0.5	0.989011	0.01087
	3.2	0.875	0.978528	0.021407
	1.6	0.75	0.988764	0.011194
	0.8	0	1	0
	0.4	0	1	0
	0.2	0	0	0

Station CYVC	Visibility Range	POD	FAR	CSI X
	9.6	0	1	0
	8	0	1	0
	6.4	0	1	0
	4.8	1	0.987013	0.012987
	3.2	1	0.990521	0.009479
	1.6	1	0.992308	0.007692
	0.8	0	1	0
	0.4	0	1	0
	0.2	0	0	0

Station	Visibility			
CYVQ	Range	POD	FAR	CSI X
	9.6	0.222222	0.988571	0.010989
	8	0.1	0.992908	0.006667
	6.4	1	0.985075	0.014925
	4.8	0.857143	0.977778	0.02214
	3.2	1	0.995828	0.004172
	1.6	1	0.998654	0.001346
	0.8	0.666667	0.997899	0.002099
	0.4	1	0.995341	0.004659
	0.2	0	0	0

Station	Visibility			
CYZF	Range	POD	FAR	CSI X
	9.6	0.333333	0.993151	0.006757
	8	0	1	0
	6.4	0	1	0
	4.8	0.666667	0.995086	0.004902
	3.2	1	0.998691	0.001309
	1.6	1	0.989535	0.010465
	0.8	1	0.998336	0.001664
	0.4	1	0.993318	0.006682
	0.2	0	0	0

Station	Visibility			
CYEV	Range	POD	FAR	CSI X
	9.6	0.142857	0.962963	0.030303
	8	0	1	0
	6.4	0	1	0
	4.8	1	0.960784	0.039216
	3.2	0.4	0.933333	0.060606
	1.6	0.875	0.934579	0.064815
	0.8	1	0.944444	0.055556
	0.4	1	0.988235	0.011765
	0.2	0	0	0

Station	Visibility			
CYPA	Range	POD	FAR	CSI X
	9.6	0	1	0
	8	0	1	0
	6.4	0	1	0
	4.8	0	1	0
	3.2	0	1	0
	1.6	0	1	0
	0.8	0	1	0
	0.4	0	1	0
	0.2	0	0	0

Station	Visibility			
CYXY	Range	POD	FAR	CSI X
	9.6	0	1	0
	8	1	0.994764	0.005236
	6.4	0.333333	0.996815	0.003165
	4.8	0.2	0.997972	0.002012
	3.2	0.625	0.994206	0.005774
	1.6	0.6	0.997178	0.002817
	0.8	0.5	0.998855	0.001144
	0.4	0	1	0
	0.2	0	0	0

Arctic eco-climatic zone

Station	Visibility			
CYCO	Range	POD	FAR	CSI X
	9.6	0.333333	0.982759	0.016667
	8	0	1	0
	6.4	0.333333	0.994318	0.005618
	4.8	0	1	0
	3.2	0.272727	0.994624	0.0053
	1.6	0.45	0.990605	0.009288
	0.8	0.607143	0.9895	0.010429
	0.4	0.873171	0.933358	0.066003
	0.2	0	0	0

Station	Visibility			
CYBK	Range	POD	FAR	CSI X
	9.6	0.214286	0.993789	0.006073
	8	0.1	0.99812	0.001848
	6.4	0.333333	0.995652	0.00431
	4.8	0.538462	0.987037	0.012821
	3.2	0.473684	0.987629	0.012203
	1.6	0.555556	0.988493	0.011403
	0.8	0.503759	0.983042	0.016679
	0.4	0.858997	0.903653	0.094847
	0.2	0	0	0

Station	Visibility			
CYRB	Range	POD	FAR	CSI X
	9.6	0.1	0.996587	0.003311
	8	0	1	0
	6.4	0.166667	0.992537	0.007194
	4.8	0.428571	0.991781	0.00813
	3.2	0.538462	0.974592	0.024867
	1.6	0.77551	0.978047	0.021814
	0.8	0.782609	0.987166	0.012789
	0.4	0.90932	0.976458	0.023487
	0.2	0	0	0

Station	Visibility			
CYYQ	Range	POD	FAR	CSI X
	9.6	0.125	0.994536	0.005263
	8	0	1	0
	6.4	0	1	0
	4.8	0	1	0
	3.2	0.882353	0.986162	0.013812
	1.6	0.851852	0.986334	0.013634
	0.8	0.863636	0.982383	0.017568
	0.4	0.895307	0.956959	0.042825
	0.2	0	0	0

Station	Visibility			
CYCB	Range	POD	FAR	CSI X
	9.6	0.166667	0.985765	0.013289
	8	0.166667	0.994361	0.005484
	6.4	0.083333	0.99537	0.004405
	4.8	0.411765	0.980226	0.019231
	3.2	0.48913	0.962717	0.035885
	1.6	0.566667	0.980516	0.019198
	0.8	0.669643	0.972036	0.027584
	0.4	0.922664	0.904183	0.095054
	0.2	0	0	0

Station	Visibility			
CYFB	Range	POD	FAR	CSI X
	9.6	0.181818	0.985375	0.013722
	8	0	1	0
	6.4	0.166667	0.987952	0.011364
	4.8	0.265306	0.978405	0.020376
	3.2	0.666667	0.976235	0.023486
	1.6	0.75	0.981489	0.018397
	0.8	0.701754	0.987253	0.012678
	0.4	0.855204	0.978236	0.021684
	0.2	0	0	0

Station	Visibility			
CYIO	Range	POD	FAR	CSI X
	9.6	0.0625	0.997608	0.002309
	8	0.2	0.99005	0.009569
	6.4	0.333333	0.995169	0.004785
	4.8	0.1	0.997797	0.00216
	3.2	0.333333	0.991172	0.008675
	1.6	0.295455	0.994263	0.00566
	0.8	0.263158	0.997202	0.002776
	0.4	0.472222	0.997273	0.002718
	0.2	0	0	0

Station	Visibility			
CYTE	Range	POD	FAR	CSI X
	9.6	0	1	0
	8	0.136364	0.973451	0.022727
	6.4	0	1	0
	4.8	0.181818	0.987421	0.011905
	3.2	0.553571	0.945326	0.052365
	1.6	0.645161	0.972973	0.026631
	0.8	0.730769	0.980311	0.019547
	0.4	0.944444	0.971556	0.028396
	0.2	0	0	0

Station	Visibility			
CYUX	Range	POD	FAR	CSI X
	9.6	0.111111	0.990476	0.00885
	8	0.142857	0.992754	0.006944
	6.4	0	1	0
	4.8	0.545455	0.986517	0.013333
	3.2	0.542056	0.966686	0.032402
	1.6	0.612245	0.976888	0.022779
	0.8	0.816832	0.956303	0.043273
	0.4	0.961278	0.903065	0.096558
	0.2	0	0	0

Station	Visibility			
CYZS	Range	POD	FAR	CSI X
	9.6	0.2	0.993878	0.005976
	8	0.125	0.99651	0.003407
	6.4	0.5	0.996441	0.003546
	4.8	0.333333	0.986765	0.012894
	3.2	0.264151	0.991479	0.008323
	1.6	0.514019	0.982639	0.017081
	0.8	0.553672	0.972143	0.027245
	0.4	0.980375	0.885102	0.114634
	0.2	0	0	0

Mountain eco-climatic zone

Station CYQF	Visibility Range	POD	FAR	CSI X
	9.6	0	1	0
	8	0	1	0
	6.4	0	1	0
	4.8	0	1	0
	3.2	1	0.994778	0.005222
	1.6	1	0.997319	0.002681
	0.8	0	1	0
	0.4	1	0.985455	0.014545
	0.2	0	0	0

Station CYXH	Visibility Range	POD	FAR	CSI X
	9.6	1	0.986111	0.013889
	8	0	1	0
	6.4	0	1	0
	4.8	1	0.979167	0.020833
	3.2	0	1	0
	1.6	1	0.994819	0.005181
	0.8	1	0.990521	0.009479
	0.4	0	1	0
	0.2	0	0	0

Station CYYC	Visibility Range	POD	FAR	CSI X
	9.6	0	1	0
	8	0	1	0
	6.4	0	1	0
	4.8	0	1	0
	3.2	0	1	0
	1.6	1	0.99536	0.00464
	0.8	0	1	0
	0.4	1	0.993921	0.006079
	0.2	0	0	0

Station CYEG	Visibility Range	POD	FAR	CSI X
	9.6	0	1	0
	8	0	1	0
	6.4	0	1	0
	4.8	0	1	0
	3.2	1	0.997642	0.002358
	1.6	1	0.997712	0.002288
	0.8	0	1	0
	0.4	1	0.916667	0.083333
	0.2	0	0	0

References

Baggaley, D. G. and Hanesiak J. M., 2005: An empirical Blowing Snow Forecast Technique for the Canadian Arctic and the Prairie Provinces. *Weather and Forecasting*, **20**, 51-62.

Conklin, M. H., and R. C. Bales, 1993: SO_2 Uptake on Ice Spheres: Liquid nature of the Ice-Air Interface. *Journal of Geophysical Research*, **98**(D9)

Deming, J., T. Papakyriakou, J. Yackel, P. Taylor, C. Blouw, C. Breneman, J. Butler, A. Langlois, O. Owens, R. Pierson, S. Savelyev, M. Suitor, 2004: CASES2004, Leg 4 Cruise Report. *Ice-Atmosphere Interactions and Biological Linkages*, Webpage: http://www.cases.quebec-ocean.ulaval.ca/CASES0304_leg4_cruise_report(partial).pdf, 2-6

Déry, S. J., 2004: Technical Details of the PIEKTUK Blowing Snow Model. Webpage: http://web.unbc.ca/~sdery/datafiles/piektuk2.htm

Déry, S. J., Taylor, P. A., and Xiao J., 1998: The Thermodynamic Effects of Sublimating Snow in the Boundary Layer. *Boundary-Layer Meteorology*, **89**, 251-283.

Déry, S. J. and M. K. Yau, 1999: A Bulk Blowing Snow Model. *Boundary-Layer Meteorology*, **93**, 237-251.

Déry, S. J. and M. K. Yau, 2001a: Simulation of an Arctic Ground Blizzard Using a Coupled Blowing Snow-Atmospheric Model. *Journal of Hydrometeorology*, **2**, 579-598.

Déry, S. J. and M. K. Yau, 2001b: Simulation of Blowing Snow in the Canadian Arctic Using a Double-Moment Model. *Boundary-Layer Meteorology*, **99**, 297-316.

Hanesiak, J, 2002: Personal Conversation

Huang, Q., J. Hanesiak, S. Savelyev, T. Papakyriakou, and P. Taylor, 2007: Visibility During Blowing Snow Events Over Arctic Sea Ice. In process.

Li, L., and J. W. Pomeroy, 1997a: Estimates of Threshold Wind Speeds for Snow Transport Using Meteorological Data. *Journal of Applied Meteorology*, **36**(3), 205-213.

Li, Long, and J. W. Pomeroy, 1997b: Probability of Occurrence of Blowing Snow. *Journal of Geophysical Research*, **102**, (D18), 21,995-21,964.

Mann, G. W., P. S. Anderson, and S. D. Mobbs, 2000: Profile Measurements of Blowing Snow at Halley, Antarctica. *Journal of Geophysical Research*, **105**(D19), 24,491-24,508.

MANOBS, Environment Canada, 1990: Manual of Surface Weather Observations. User's Manual. [Available from Meteorological Service of Canada, 4905 Dufferin St, Downsview, ON, M3H 5T4, Canada] 2-1 – 3-8

Ôura, H., T. Ishida, D. Kobayashi, and T. Yamada, 1967: Studies on Blowing Snow Part II. *Physics of Snow and Ice: Int. Conf. on Low Temperature Science*, Sapporo, Japan, Institute of Low Temperature Science, Hokkaido University, 1099-1117.

Pomeroy, J. W., and B. E. Goodison, 1997: Winter and Snow. *The Surface Climates of Canada*, Chapter 4, 68-100.

Pomeroy, J. W., and D. H. Male, 1988: Optical Properties of Blowing Snow. *Journal of Glaciology*, **34**(116), 3-10.

Xiao, J., R. Bintanja, S. J. Déry, G. W. Mann, P. A. Taylor, 2000: An Intercomparison Among Four Models of Blowing Snow. *Boundary-Layer Meteorology*, **97**, 109-135.